Contribution of Ketone Oxidation on Energy Production in the Failing Heart

by

Simran Ajay Pherwani

A thesis submitted in partial fulfillment of the requirements for the degree of

Master of Science

Medical Sciences - Pediatrics
University of Alberta

Abstract

One third of all deaths in Canada are due to cardiovascular diseases, including heart failure. Cardiovascular diseases have a considerable economic burden, and drastically impact the health and quality of life of Canadians. Heart failure (HF) is a clinical condition where the heart is unable to adequately pump blood throughout the body, limiting nutrient and 02 delivery. Individuals with type 2 diabetes (T2D) are at high risk of developing HF. A class of anti-diabetic drugs, sodium glucose co-transporter 2 inhibitors (SGLT2i), have recently been shown to improve HF outcomes in clinical trials with individuals with HF regardless of the presence of type 2 diabetes (T2D). SGLT2i are expressed in the proximal tubule of the kidney and are involved in 90% of the reabsorption of filtered glucose. SGLT2 inhibition prevents glucose reabsorption and reentry into the circulation, improving glycemic control. The EMPAREG-OUTCOMES trial in 2019 showed that the SGLT2i, empagliflozin, decreased hospitalization and deaths due to cardiovascular causes such as HF in T2D patients at high risk for cardiovascular events. The DAPA-HF trial in 2020 showed that the SGLT2i, dapagliflozin, also improved cardiac outcomes; however, in both the presence or absence of T2D. This was followed shortly after by the EMPEROR trial in 2021 which confirmed these observations with empagliflozin. However, it has not yet been fully established how exactly SGLT2i act to improve cardiac function, and the mechanisms responsible for their cardioprotective effects remain unclear. The failing heart exhibits a decrease in mitochondrial oxidative phosphorylation, namely glucose oxidation rates, resulting in decreased energy production in the heart. Increased evidence has shown that circulating ketones as well as cardiac ketone utilization increases in heart failure. Additionally, SGLT2i have been shown to increase circulating ketone levels. Therefore, we hypothesized that SGLT2i improve cardiac function by providing the failing heart with an extra

source of fuel in the form of ketones. Thus, the purpose of this study was to determine whether increased energetics through providing ketones as an extra fuel to the failing heart is responsible for the improvement in cardiac function and cardiovascular outcomes seen in SGLT2i clinical trials, and to address a possible mechanism behind the cardioprotective effects. 8-week old C57BL6/N mice underwent a transverse aortic constriction (TAC) or sham surgery to induce pressure overload hypertrophy over 3 weeks, following which mice were randomized to receive either dapagliflozin (1mg/kg BW) or not in their drinking water for 4 weeks. Biweekly body weight and blood glucose and ketone measurements were taken. Echocardiography was done at 3 weeks and 6 weeks post surgery to assess cardiac function, and a glucose tolerance test (GTT) was done at the 6-week time point. After the 7-week protocol, mice were subjected to ex-vivo isolated working heart perfusions, where their hearts were perfused with radiolabelled Betahydroxybutyrate (BOHB), palmitate, or glucose to assess substrate oxidation and glycolytic rates. Hearts were perfused at physiological conditions of these substrates as well as concentrations seen following treatment (i.e. BOHB levels observed *in vivo* with Dapagliflozin treatment): this was 0.2 mM and 0.6 mM BOHB, respectively. Protein expression of ketone oxidation enzymes, as well as inflammation markers in the mouse heart were measured using immunoblotting. We did not observe an improvement in *in vivo* cardiac function; however, we did observe an increase in cardiac efficiency with DAPA treatment in HF, alongside increased ATP production due to increased glucose and BOHB oxidation rates. Additionally, we did not observe any significant improvement in circulating ketone levels with treatment, or in cardiac energy metabolism with dapagliflozin treatment at both 0.2 mM and 0.6 mM BOHB. Therefore, our results suggest that the beneficial cardiovascular effects of SGLT2i may not be due to fuel use and improved energetics as hypothesized, as we did not observe any significant changes in

substrate oxidative rates with dapagliflozin. Since we observed a trend towards an increase in NLRP3/NALP3 inflammasome protein expression, we believe there is value in exploring the NLRP3/NALP3 inflammasome pathway as a potential mechanism through which SGLT2i may be acting.

Preface

This thesis is an original work by Simran Ajay Pherwani. No part of this thesis has been previously published. The research project, of which this thesis is a part of, received research ethics approval from the University of Alberta Research Ethics Board, Project Name "Protection of the ischemic myocardium", AUP00000288_AME22, July 9, 2013 (most recent renewal March 6, 2021).

Some of the techniques in this research study were conducted by other personnel. Transverse aortic constriction (TAC) surgeries and echocardiography were done by lab technicians from the Dyck lab, Jody Levasseur and Heidi Silver, respectfully. Ex-vivo isolated working heart perfusions were done by the lab technician from the Lopaschuk Lab, Cory Wagg.

Acknowledgements

First and foremost, I sincerely thank my supervisor, Dr. Gary Lopaschuk, for his unparalleled mentorship and guidance, and for the immense diverse opportunities he provided me to excel in my MSc degree. Thank you for supporting my professional growth, challenging me to think critically, and never give up in times of difficulty (as well as answering my stream of never ending questions!). You are an inspiration and role model to me.

I would like to express my gratitude towards my committee members, Dr. John R. Ussher and Dr. Richard Lehner for their valuable time, guidance, and thoughtful feedback.

Thank you to my fellow lab members Kim Ho, Qutuba Karwi, Liyan Zhang, Ezra Ketema, Kaya Persad, Donna Andre, and Cory Wagg for their encouragement, never-ending laughs, and friendship. I would like to thank my summer student and Physiology Honors project student David Connolly for his help and support throughout the project, especially during troubleshooting, and for helping me develop into a strong mentor.

I would like to thank my parents, Lata and Ajay Pherwani, for your love, encouragement, and support throughout my life and MSc degree. I also want to thank 2 of my close friends, Rebecca Yang and Amy Nowakowsky, for being my biggest cheerleaders and never letting me give up.

Table of Contents

List of Tables

.

List of Figures

List of Abbreviations

Abbreviation	Definition
AMPK	AMP-activated protein kinase
ACC	Acetyl-CoA carboxylase
AcAc	Acetoacetate
Ac-CoA	Acetyl-CoA
ANOVA	Analysis of variance
ATP	Adenosine triphosphate
AU	Arbitrary units
BDH-1	BOHB dehydrogenase
BHAD	Beta-hydroxyacyl-CoA dehydrogenase
BOHB	Beta-hydroxybutyrate
BSA	Bovine serum albumin
CPT-1	Carnitine palmitoyltransferase 1
CPT-2	Carnitine palmitoyltransferase 2
BW	Body weight
DAPA/Dapa	Dapagliflozin
DCA	Dicholoroacetate
Echo	Echocardiography
EDV	End diastolic volume
ESV	End systolic volume
ETC	Electron transport chain
FA	Fatty acid
FACS	Fatty acyl-CoA synthase
$FADH_2$	Flavin adenine dinucleotide
FFA	Free fatty acid
GLUT4	Glucose transporter type 4
HF	Heart failure

HFrEF	Heart failure with reduced ejection fraction
HFpEF	Heart failure with preserved ejection fraction
HMGCS2	3-hydroxy-3-methlyglutaryl-CoA synthase 2
HMGCL/HL	3-hydroxy-3-methlyglutaryl lyase
IL-18	Interleukin 18
IL-1B	Interleukin 1B
IVD:d	Interventricular septum thickness at end-diastole
IVD:s	Interventricular septum thickness at end-systole
IVS	Interventricular septum
KO	Knockout
LV	Left ventricle/left ventricular
LVID:d	Left ventricular internal dimension at end-diastole
LVID:s	Left ventricular internal dimension at end-systole
LVPW:d	Left ventricular posterior wall thickness at end-diastole
LVPW:s	Left ventricular posterior wall thickness at end-systole
mM	Milimoles
MCD	Malonyl-CoA decarboxylase
MI	Myocardial infarction
NADH	Nicotinamide adenine dinucleotide + hydrogen
NAD+	Nicotinamide adenine dinucleotide
NRLP3/NALP3	Nod like receptor family protien 3
P-PDH	Phosphorylated pyruvate dehydrogenase
PDH	Pyruvate dehydrogenase
PDK	Pyruvate dehydrogenase kinase

P/O ratio	Phosphate oxygen ratio
SCOT	Succinyl-CoA-3-ketoacid-CoA transferase
SD	Standard deviation
SDS-PAGE	Sodium dodecyl sulfate polyacrylamide gel electrophoresis
SEM	Standard error mean
SGLT1	Sodium glucose co-transporter 1
SGLT2	Sodium glucose co-transporter 2
SGLT2i	Sodium glucose co-transporter 2 inhibitor
TAC	Transverse aortic constriction
TCA	Tricarboxylic acid cycle
T1D	Type 1 diabetes
T2D	Type 2 diabetes
%EF	Percent ejection fraction
%FS	Percent fractional shortening

Chapter One

LITERATURE REVIEW

1.1 Literature Review

1.1.1 Overview of Heart Failure

One third of all of the deaths across the world are due to cardiovascular disease, one of the most predominant being heart failure (HF) [1-3]. Cardiovascular diseases have a considerable economic and financial burden, and drastically impact the quality of life of Canadians. [4, 5]. Patients diagnosed with HF still have a poor prognosis despite the development and use of current therapeutic and treatment approaches. HF is a complex clinical syndrome where the heart is unable to adequately pump blood throughout the body, limiting its ability to deliver proper amounts of oxygen and nutrients throughout the body [6, 7]. HF is often a result of and dependant on various risk factors and comorbidities including obesity, diabetes, inflammation, hypertension, myocardial infarction, volume overload, and common obstructive pulmonary disease [8]; therefore, HF is not one specific disease, rather it has a complex pathophysiology. It often affects individuals at older ages, and is the leading cause of hospitalization for patients over 65 years old [1-3]**.** HF can involve both systolic and diastolic left ventricular (LV) dysfunction [9-14]. There are two major types of HF categorized based on % ejection fraction (%EF): heart failure with reduced ejection fraction (HFrEF) and heart failure with preserved ejection fraction (HFpEF) [8]**.** HFrEF is defined by %EF less than 40% and involves impaired contractility and pumping of blood out of the left ventricle which results in a decreased amount of blood pumped during each contraction, and resulting systolic dysfunction. In contrast, HFpEF is characterized by %EF greater than 50% and involves impaired relaxation or filling capacity of the left ventricle without a major decrease in the amount of blood being pumped with each contraction. Each type of HF involves different underlying cellular and molecular differences.

Type 2 diabetes (T2D) is a significant as well as a major independent risk factor for the development of HF [15-17] and the prevalence of HF alongside diabetes is common among the elderly. Diabetes mellitus is a metabolic disorder characterized by hyperglycemia, increased blood glucose in circulation, resulting from either insulin deficiency or resistance, defined as

type 1(T1D) or type 2 diabetes mellitus respectively [18]. In T1D, pancreatic beta cells are destroyed by the body through an autoimmune disease state resulting in the inability to produce insulin; it is also referred to as insulin-dependant diabetes as individuals need to take insulin to regular their blood sugar levels [19]. In T2D, there is a deficit in the function of the insulin that is produced by pancreatic beta cells; this is also referred to as insulin-independent diabetes as the body is still able to produce insulin. T2D is more common and various risk factors for its development and severity include age, obesity, diet, and hypertension amongst the most common. The presence of both T2D and cardiovascular disease increases risk of cardiovascular mortality [20-23]. This has an immense impact on quality of life as management of both conditions becomes a central part of individuals' lives.

1.1.2 Cardiac Energy Metabolism in the Normal Heart

Although it has minimal energy reserves on its own [24-26], the heart has a very high energy demand and must produce large amounts of energy in the form of ATP to maintain contractile function [26]**.** The heart is able to obtain energy from the oxidation of various fuel sources, including fatty acids, carbohydrates including glucose and lactate, ketones, and branched chain amino acids [27-31] (Figure 2)**.** This makes the heart an omnivore, capable of burning each of the mentioned substrates to make ATP. This "metabolic flexibility" enables the heart to dynamically alter its preference between each fuel depending on work demand/workload, neurohormonal status, and the circulating concentration of each substrate [32-34]**.** The three main fuel sources that the heart relies on for energy are fats, carbohydrates, and ketones, and the contribution of the substrates to ATP production can dramatically be altered in different pathophysiological states, such as HF [34, 35]**.** Lactate and branched chain amino acids are not a focus in this research study; therefore, these fuel sources will not be discussed in detail in this literature review.

In the normal heart, the majority (around 95%) of ATP is produced from mitochondrial oxidative phosphorylation, primarily from the oxidation of fatty acids and carbohydrates, alongside other substrates, while a small remainder is derived from glycolysis [26, 33, 35, 36] (Figure 1 and 2). Each of these substrates produces Acetyl-CoA which feeds into the Tricarboxylic acid (TCA) cycle (Figure 1). Mitochondrial oxidative phosphorylation involves the production of reduced

equivalents, NADH and $FADH_2$ from the pyruvate dehydrogenase reaction, B-oxidation, and the TCA cycle from carbon-based substrates. Each turn of the TCA cycle produces 3 NADH, 1 FADH2 and 1 ATP [26]. These equivalents release electrons to the electron transport chain (ETC) in the inner mitochondrial membrane to create ATP from ATP synthase, through chemiosmosis. An increase in contractile force increases the production of ATP from mitochondrial oxidative phosphorylation [26]. The rates of flux through the various metabolic pathways are controlled by the expression of metabolic enzymes in those pathways alongside allosteric regulation and end-product inhibition. This allows for adaption to various acute stress states, such as exercise, fasting, ischemia, or change in substrate circulating concentrations.

1.1.2.1 Fats

Fats serve as the major source of ATP and Acetyl-CoA in the heart, contributing around 40-60% of total cardiac energy production through B-oxidation [34] (Figure 2)**.** Circulating free fatty acids bound to albumin and fatty acids liberated from triglycerides are transported into the cardiomyocyte through diffusion through the plasma membrane or CD36 transporters [35, 37]. Once inside the cytosol, they are esterified to form triacylglycerol, or the fatty acids are esterified into long chain fatty acyl CoA esters by fatty acyl CoA synthase (FACS). These fatty acyl CoA's are converted to long chain acylcarnitine by carnitine palmitoyltransferase (CPT) 1 (CPT1) in the outer mitochondrial membrane. CPT1 can be regulated by allosteric inhibition by malonyl CoA, which is synthesized from Acetyl-CoA by Acetyl-CoA carboxylase (ACC) and broken down by malonyl CoA decarboxylase (MCD). AMPK phosphorylates and inactivates ACC, resulting in higher fatty acid oxidation and lower inhibition. The acylcarnitine is transported into the mitochondria and converted back into fatty acyl CoA by CPT2, which then enters the B-oxidation cycle (Figure 1).

Each cycle of fatty acid B-oxidation results in the shortening of the fatty acyl CoA molecule by 2 carbons, and the production of Acetyl-CoA, NADH, and $FADH_2$, which enter the TCA cycle and the ETC [35, 37]. The B-oxidation pathway enzymes exist in various isoforms specific to various fatty acyl CoA molecule chain lengths. The pathway is controlled by concentrations of Acetyl-CoA, NADH, and $FADH_2$ through feedback and product inhibition, as well as work demand and oxygen supply to the heart. An increase in fatty acid oxidation is accompanied by a decrease in

glucose oxidation due to the Randle cycle, through which an increase or decrease in the oxidation of one of these substrates results in the opposite change in the oxidation rate of the other substrate [38]. An increase in PDH activity can inhibit B-oxidation. Fatty acids carry more reducing equivalents than glucose [37], and the complete oxidation of the fatty acid palmitate produces 105 ATP per fatty acid molecule [35]. Oxidation of fatty acids produces more ATP per molecule than any other energy substrate; however, this consumes more oxygen, making fatty acids a very inefficient source of energy.

1.1.2.2 Carbohydrates

Carbohydrates: glucose and lactate, make up the second largest fuel source in the normal heart [34] (Figure 2). Glycolysis and lactate oxidation contribute a small amount to total energy production, around 2-8% and 10-15% respectively, while the majority of ATP from carbohydrates is produced through glucose oxidation, around 20-40%. Glucose is taken up into the cardiomyocytes and is used as a substrate for glycolysis, an anaerobic process occurring in the cytosol, to form 2 3-carbon pyruvate molecules [37] (Figure 1). The pyruvate produced from glycolysis can have 2 fates; it can either be converted and reduced into lactate, or further oxidized in the mitochondria. Glycolysis produces 2 ATP from substrate level phosphorylation and 2 NADH per glucose molecule, which feeds into the TCA cycle in the presence of oxygen, or is converted to NAD+ in the absence of oxidation alongside the reduction of pyruvate into lactate [39]. Pyruvate can be converted and decarboxylated to Acetyl-CoA through the pyruvate dehydrogenase (PDH) reaction, which is the key irreversible step and produces 1 NADH molecule per pyruvate [26]. PDH is the rate limiting enzyme of glucose oxidation, and can be phosphorylated and inhibited by pyruvate dehydrogenase kinase (PDK) [26]; PDK4 is the predominant form in the heart [40]. The Acetyl-CoA produced from the PDH reaction feeds into the TCA cycle, and there are 2 turns of the cycle for every glucose molecule [26] (Figure 1). Glucose oxidation produces approximately 30 ATP per glucose molecule.

1.1.2.3 Ketones

Ketone bodies are also an important fuel source in the heart, although they are not one of the two major fuel sources [27, 41]. Ketone oxidation accounts for around 10-15% of energy production in the normal heart [34] (Figure 2). There are three main ketone bodies: B-hydroxybutyrate

(BOHB), acetoacetate (AcAc), and acetone; BOHB and AcAc are the most abundant, while acetone is low in abundance, exhaled, and responsible for the "sweet" breath of type 2 diabetics [42].

Ketones are produced in the liver primarily during states of fasting or prolonged starvation, when there is low blood glucose [43, 44]; ketones can also be produced when consuming a high-fat diet [42]. During these states, the Acetyl-CoA produced from B-oxidation of fatty acids is converted into ketone bodies though a process known as hepatic ketogenesis [44, 45]. Thiolase converts Acetyl-CoA into Ac-Ac-Coa, and 3-hydroxymethylglutaryl-CoA synthase 2 (HMGCS2) catalyzes the condensation of Ac-Ac-Coa into HMG-CoA, which is then converted to AcAc by 3-hydroxymethylglutaryl lyase (HMGCL or HL). AcAc can be further converted to BOHB by BOHB dehydrogenase (BDH1), and also to acetone. Once they are made, ketone bodies are released from the cell via monocarboxylate transporters (MCT) [46], and travel to extra-hepatic tissues such as the brain, muscle, and heart to be oxidized and burned as fuel [44, 45, 47]. Ketone bodies are taken up by SLC16A1 and SLC16A7 transporters [48, 49], and BOHB is converted into AcAc through the BDH1 enzyme, which also produces 1 NADH molecule. AcAc is converted to acetoacetyl CoA through the succinyl-CoA:3-oxoacid-CoA transferase (SCOT) enzyme, which also produces succinate from succinyl CoA, and this acetoacetyl-CoA is converted finally to Acetyl-CoA by the thiolase enzyme to feed into the TCA cycle. SCOT is the rate limiting enzyme of ketone oxidation (Figure 1).

Plasma circulating ketone concentrations are normally < 1 mM mM in the postprandial or fed state [50], but can reach upto 6 mM during prolonged fasting [50] and 25 mM in uncontrolled diabetes [51]. In the fed state, ketogenesis is inhibited due to inhibiting hormone-sensitive lipase, preventing the breakdown of triacylglycerols [52]. Additionally, insulin levels are high in the fed state; high insulin levels activate ACC, increasing malonyl-CoA levels, thereby inhibiting fatty acid oxidation [53]. Ketone oxidation does not occur in the liver as it lacks the enzyme SCOT [44]. Approximately 22 ATP are produced per ketone molecule [54]. Ketone oxidation is proportional to its delivery and supply, and circulating ketone concentration is an important determinant of myocardial ketone oxidation rates [43, 44, 55-57]. Ketone oxidation is regulated by both transcriptional and post-transcriptional modification [58-61]. Ketone bodies also serve

other roles that are non-metabolic based, including as signalling molecules [62, 63], as anti-hypertrophic agents through histone deacetylase inhibition [64, 65], and as modulators in inflammation and oxidative stress [66-68].

Although this substrate does not contribute a large amount towards ATP production in the normal heart, it may serve as an additional source of energy for the energy starved failing heart, which will be described below in the next section.

1.1.3 Metabolic Perturbations in the Failing Heart

The failing heart exhibits impaired metabolic flexibility [69], and there are profound alterations in cardiac energy metabolism and bioenergetics [35, 36]. *In vivo* measurements of cardiac phosphocreatine and ATP using ^{31}P-NMR spectroscopy in the myocardium showed a decreased phosphocreatine/ATP ratio in the human failing heart, and ATP production is estimated to be reduced by upto 40% in the failing heart compared to in the normal heart [70-72]. This is a result of impairment in the ETC and mitochondrial function [73, 74], alongside dramatic changes in energy substrate preferences [75-77]. In HF, there is a decrease in cardiac mitochondrial oxidative metabolism namely glucose oxidation, and glycolysis is uncoupled from glucose oxidation (Figure 2). This results in an "energy starved" state for the failing heart [35, 72], as the failing heart is referred to as "an engine out of fuel" [72, 78, 79], and this may contribute to the severity of heart failure and contractile dysfunction. Together, this results in an inefficient heart and functional impairment in heart failure [80-82].

Optimizing energy substrate use through pharmacological interventions has emerged as a promising potential approach to decrease the severity of heart failure and improve cardiac efficiency [34]. This is namely through increasing cardiac mitochondrial glucose oxidation, or by decreasing cardiac mitochondrial fatty acid oxidation. Circulating ketones and their subsequent oxidation have also shown to be increased in heart failure, and have shown to be a possible therapeutic approach beneficial in HF.

1.1.3.1 Fats

Under aerobic conditions, the heart derives the majority of its energy requirements from the oxidation of fatty acids and glucose [26, 31, 34, 35] (Figure 2). However, with the significant decrease in mitochondrial glucose oxidation, the failing heart must rely on the oxidation of a very energy inefficient fuel source. Additionally, early stages of heart failure lead to increased lipolysis, resulting in increased circulating concentrations of fatty acids and the subsequent increase in fatty acid oxidation [83-86]. Increased fatty acid uptake is also observed [87, 88]. However, there is not a uniform consensus as to what happens to cardiac fatty acid oxidation in heart failure. Both human and animal studies have shown fatty acid oxidation to increase [89, 90], decrease [91-94], or have no significant change [95-97] in heart failure. However, an improvement in cardiac efficiency and function has been observed through inhibiting cardiac mitochondrial fatty acid oxidation in the failing heart [32, 35, 72, 98].

1.1.3.2 Carbohydrates

Cardiac mitochondrial oxidative phosphorylation is significantly lower in the failing heart; this is namely due to a dramatic reduction in mitochondrial glucose oxidation [26, 34, 35] (Figure 2). This impairment in glucose oxidation is though to be due to impaired mitochondrial oxidative capacity and reduced expression and activity of PDH [99, 100]. Moreover, expression of the glucose transporter GLUT4 is reduced [101]. Glycolysis rates have been shown to increase in both animal [102, 103] and human models of HF [104]**.** Additionally, glucose oxidation is uncoupled from glycolysis, resulting in an increased proton production, generating heat [105], alongside impaired contractility [106].

Optimizing energy substrate utilization, particularly by increasing mitochondrial glucose oxidation, can be a potentially promising approach to decreasing the severity of heart failure by increasing total energy production in the failing heart and improving cardiac efficiency [34, 75]. This may serve as a possible therapeutic approach for patients with HF. Stimulation of glucose oxidation through dicholoroacetate (DCA) has been shown to promote myocardial glucose oxidation at the expense of myocardial fatty B-oxidation, through stimulating the mitochondrial PDH complex by directly inhibiting the activity of PDK [107, 108]**.** Decreasing cardiac mitochondrial fatty acid oxidation can also be another strategy that can increase cardiac

mitochondrial glucose oxidation through the Randle cycle. Several CPT1 inhibitors have drawn recent attention in being able to increase myocardial glucose oxidation through inhibiting mitochondrial fatty acid uptake [109-111]. Another approach to inhibiting fatty acid oxidation is directly inhibiting B-oxidation rather than targetting uptake. Trimetazidine is a treatment which inhibits an enzyme in the B-oxidation pathway [112], and has shown to increase glucose oxidation [113]. MCD inhibitors are also being used to increase malonyl CoA and stimulate glucose oxidation secondary to inhibiting CPT1 [114-116].

1.1.3.3 Ketones

Recent evidence has shown that circulating ketone body levels and the capacity of the failing heart to oxidize ketone bodies is increased. In the late 1990's, Lommi et al. observed an increase in circulating concentrations of ketone bodies in patients with heart failure proportionally to the severity of cardiac dysfunction [117]**.** Various other studies in human patients with HF also found similar results, including an increased serum to myocardial ratio of ketone bodies [118], increased uptake of ketone bodies in HF [119], and upregulation of ketone body oxidation enzymes in patients with HF vs non heart failure controls [118]**.** This was also shown in animal models, where mass spectrometry based quantitative proteomics showed that BDH1, a major enzyme involved in ketone body oxidation, was upregulated in compensated hypertrophy and HF mice compared to sham mice [120]**.** Together, these findings suggest an increase reliance on ketone body oxidation as a fuel for the failing heart.

The role of ketones in cardiac energy production is increasingly becoming recognized, and ketones can provide an extra source of fuel for the starving failing heart. Altering ketone oxidation may be a beneficial therapeutic strategy to aid the failing heart. However, it is debated whether this increase in circulating ketones and ketone oxidation is adaptive or maladaptive for the failing heart. A cardiac specific SCOT KO caused increased pathological remodelling in a mouse model of pressure overload injury [121], suggesting that without the main ketone body oxidation enzyme present, the prevention of ketone body oxidation may have adverse effects, supporting an adaptive effect of ketones in HF. Additionally a human study showed that increased delivery of ketone bodies in chronic heart failure patients increased ejection fraction, cardiac function, and myocardial oxygen consumption, suggesting that increasing ketone bodies

through ketone infusions may be a potential treatment in heart failure patients [122]. This was supported by a study in tachycardia-induced cardiomyopathy dogs which showed BOHB infusion significantly improved systolic dysfunction and LV remodelling [123]. In the same vein, ketone esters have also emerged as a potential therapeutic strategy to increase ketone levels in circulation and subsequent ketone oxidation in HF [124]. Together, evidence points in the direction that increased ketone oxidation may be an adaptive strategy in HF; however, whether this is beneficial or adverse is still a topic of controversy and yet to be completely elucidated.

While ketone oxidation has widely been touted as a "thrifty" or "superfuel" for the heart [125, 126], ketones, although they are a more efficient fuel source than fatty acids, are not a more energy efficient fuel source than glucose [31]. The phosphate/oxygen (P/O) ratio is a measure of the efficiency of a fuel substrate, and the P/O ratio is 2.58 for glucose, 2.5 for ketones, and 2.33 for fatty acids. Ketone oxidation does not improve cardiac efficiency in the heart, as shown by our previous studies [80, 127]. A human study in which heart failure patients were infused with BOHB showed that increasing circulating ketone body levels did not increase cardiac efficiency, supporting our work [122]. Therefore, although increased ketone oxidation can benefit the energy starved failing heart, ketones are an extra source of fuel, not a superfuel.

1.1.4 Sodium Glucose Co-Transporter 2 Inhibitors (SGLT2i)

Sodium glucose co-transporter 2 (SGLT2) is expressed in the proximal tubule of the kidney and is involved in 90% of the reabsorption of filtered glucose [128] (Figure 3)**.** SGLT2i inhibition through inhibitors, such as empagliflozin, dapagliflozin, and canaflagozin, prevent glucose reabsorption in the kidneys and its re-entry into the circulation, causing glucose to be excreted in the urine and an improvement in glycemic control [129]. These anti-diabetic drugs are very beneficial in the management of T2D, and work independently of insulin [130]**.** In addition to reducing hyperglycemia, SGLT2i also reduce blood pressure [131] and body weight [132] (Figure 3)**.** The reduction in body weight is associated with increased lipolysis and fatty acid oxidation [133]**.** SGLT2i are originally used as an anti-diabetic drug to treat diabetes, as they have beneficial effects in T2D patients in improving glycemic control [134]. Three SGLT2i approved for clinical use are empagliflozin, dapagliflozin, and canagliflozin, and they are marketed as Jardiance, Forxiga, and Invokana, respectively.

1.1.5 SGLT2i Cardioprotection and Proposed Mechanisms

Recently, large multicentre double-blind randomized placebo-controlled trials have shown SGLT2i to improve cardiovascular outcomes in both T2D and non-diabetic patients at high risk for cardiovascular events. The EMPA-REG OUTCOMES trial showed a lower occurrence of death from cardiovascular causes, nonfatal myocardial infarction (MI), or nonfatal stroke, and a reduction in overall mortality and heart failure hospitalization in empagliflozin treated T2D patients with cardiovascular risk compared to placebo [135]. The CANVAS and DECLARE-TIMI trials supported the results of the study with Canagliflozin [136] and Dapagliflozin [137]. Interestingly, very recently, the DAPA-HF trial showed a reduction of in the risk of mortality and HF reduction in patients with HFrEF with or without T2D [138]. This was followed shortly by supporting results seen with empagliflozin in the EMPEROR-Reduced trial [139]. Therefore, SGLT2 inhibition has beneficial effects beyond T2D, in non T2D HF patients as well as T2D patients. Additionally, animal studies have also demonstrated SGLT2 inhibition to ameliorate cardiac dysfunction in mouse [140], rat [141], and pig models [142] of non-diabetic HF.

However, despite these beneficial cardiovascular outcomes, it has not yet been fully established how exactly SGLT2i act to improve cardiac function. Multiple mechanisms have been proposed to explain the benefits; however, a single mechanism has not been elucidated and it is still unclear how these benefits occur. Amongst the proposed mechanisms is the diuretic and natriuretic theory that proposes that SGLT2i are beneficial secondary to their effects on blood pressure [135, 143, 144]**.** The significant increase in urinary sodium excretion seen with SGLT2i have a diuretic effect leading to greater fluid loss, and subsequently lower blood pressure with SGLT2i. Decreasing blood pressure has beneficial effects on cardiac workload, which can improve arterial coupling and cardiac efficiency**.** Inflammation plays a significant role in the development and progression of heart failure, and SGLT2i have shown to increase circulating ketone levels which has been linked to suppression of the IL-1B pathway [145]. Studies have shown SGLT2i to attenuate cardiac fibrosis and collagen synthesis through the reactive oxygen and nitrogen (RONS)/STAT3-depandant pathway [146], and also significantly attenuate cell-mediated extracellular matric collagen remodelling [147]. SGLT2i also have shown to exert anti-inflammatory effects through the nod-like receptor family protein 3 (NLRP3) inflammasome [148].

As described above, the failing heart has a "starved" energy profile with decreased energy production [26, 31, 35]. SGLT2i have been shown to increase ketone body levels in the bloodstream secondary to mobilizing adipose tissue fatty acids which are used by the liver for ketogenesis [133, 149-151]**.** Therefore, perhaps, SGLT2i may be acting to improve cardiac function and outcomes through increasing ketone bodies and providing the failing heart with an extra source of energy that it can use to produce ATP. SGLT2i are not located in cardiomyocytes [152], letting this increase in circulating ketones serve as a possible mediator of the benefits. Experimental studies have suggested that increasing ketone delivery to the failing heart may improve mitochondrial function and the response to oxidative stress [123]. A study recently showed increased delivery of BOHB ameliorated pathological remodelling and dysfunction in a mouse model of pressure overload/ischemic insult as well as a canine pacing model of progressive heart failure [123]. In support of SGLT2i function through ketones, animal models treated with empagliflozin have also shown beneficial metabolic changes associated with increased ketone utilization. Empagliflozin increased circulating ketone levels and the myocardial expression of ketone body transporter and oxidation enzymes, alongside increasing cardiac total ATP production, and favorably affecting cardiac function and remodelling in a non-diabetic Sprague-Dawley MI model [141]**.** Empagliflozin also ameliorated adverse cardiac remodelling, improved systolic function, and increased myocardial uptake of ketone bodies as well as the expression/activity of ketone body oxidative enzymes in a porcine model of myocardial infarction injury [142]**.** Our previous study in diabetic cardiomyopathic mice showed empagliflozin increased cardiac ketone oxidation and provided an extra source of fuel for the heart, shown by increased total ATP [127]. Combined, this evidence suggests that strategies aimed to increase myocardial BOHB utilization, including through the administration of SGLT2i, may be beneficial in improving fuel use in HF.

1.2 Rationale

In this thesis, we aim to investigate a mechanism through which Dapagliflozin may exert its cardioprotective effects in the non-diabetic failing heart. We also aim to determine whether these beneficial effects are mediated through an increase in energy supply to the starving failing heart, in the form of ketones. As SGLT2i have been shown to increase circulating ketone concentrations, we hope this method of increasing myocardial BOHB levels and utilization may

be a potential mechanism behind which SGLT2i show cardioprotection in HF patients. Our lab will be able to measure absolute substrate metabolic rates and ex vivo cardiac function using ex-vivo isolated working heart perfusions, a technique which is very rare across the globe. We will be able to determine a mechanism for the SGLT2i cardioprotective effects and assess the impact of ketone bodies on cardiac energetics, using this very direct and accurate technique where we can perfuse the heart with the concentration of ketones seen *in vivo* with chronic SGLT2i treatment.

This study was commenced around 1-2 months after the DAPA-HF trial results were published, prior to the EMPEROR-Reduced trial results being published.

1.3 Research Question and Objectives

Our research question explores whether dapagliflozin's cardioprotective effects are mediated through increased energetics through providing ketones as an additional fuel to the starved failing heart. Our objectives are to elucidate a mechanism of action of dapagliflozin, a SGLT2i, in mediating cardioprotective effects seen in patients with heart failure. This project concentrates on the role of ketones as an extra source of fuel, and will address the beneficial and adaptive effect of increasing ketone oxidation in the failing heart. We aim to achieve this using a murine model of pressure overload hypertrophy HF, induced through transverse aortic constriction (TAC), treated chronically over 4 weeks with dapagliflozin. We hope our studies can shed light on how SGLT2i act to improve cardiac function and outcomes in both diabetic and non-diabetic heart failure patients.

1.4 Hypothesis

We hypothesize that dapagliflozin will improve cardiac function in a pressure overload hypertrophy HF rodent model, and that the beneficial effects of SGLT2i in the failing heart are due to an increase in energy supply to the starving heart, in the form of ketones.

1.5 Figures

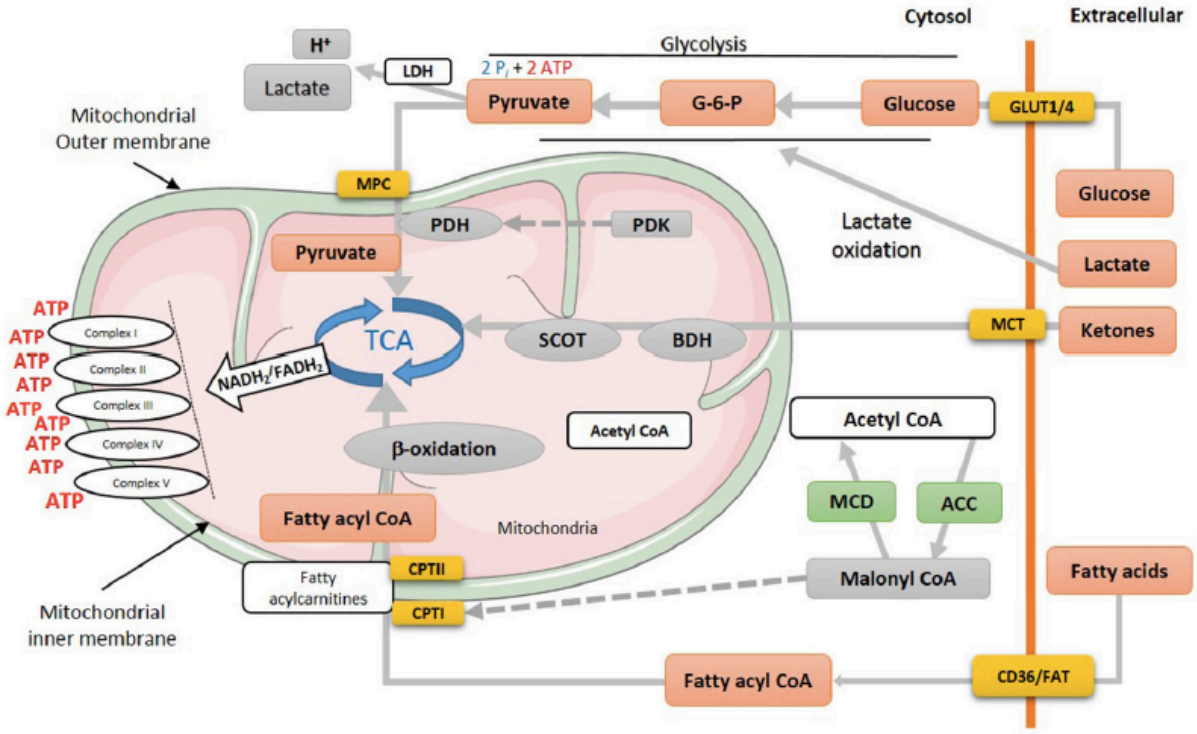

Figure 1. Overview of cardiac energy metabolism pathways. Fatty acids undergo fatty acid B-oxidation in the mitochondria. Glucose can be converted to pyruvate during glycolysis, which can either be further converted to lactate or enter the mitochondria for further oxidation. Ketones are metabolized in the mitochondria. Each pathway produces Acetyl CoA to enter the TCA cycle. Figure taken from Karwi, Q. G., Uddin, G. M., Ho, K. L., & Lopaschuk, G. D. (2018). Loss of metabolic flexibility in the failing heart. *Frontiers in cardiovascular medicine*, *5*, 68.

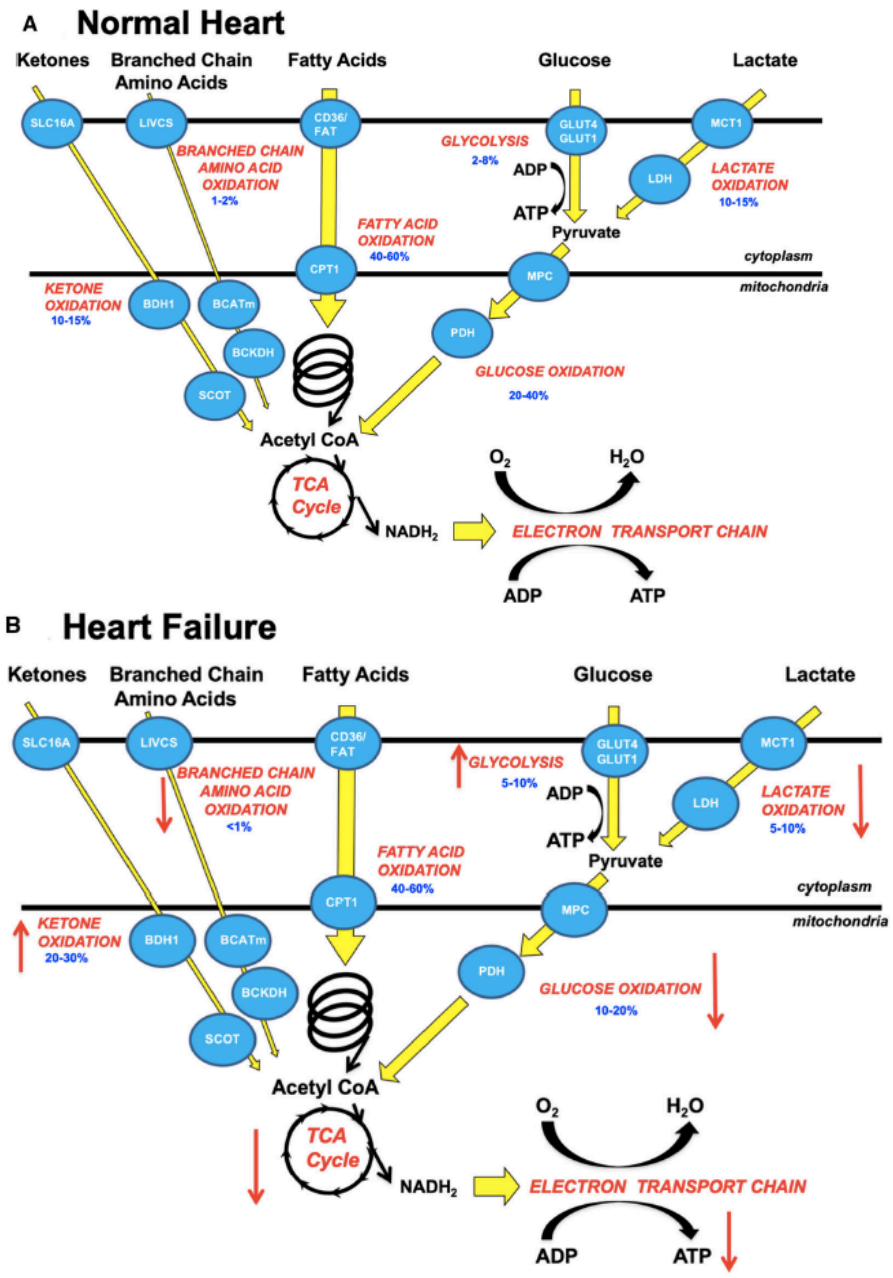

Figure 2. Cardiac energy metabolism in the normal and failing heart. The majority of ATP in the heart comes from oxidative phosphorylation, where fatty acid oxidation is the largest contributor followed by glucose oxidation. In the failing heart, there is a significant impairment in glucose oxidation; glycolysis and ketone oxidation increase, while fatty acid oxidation may stay the same. Figure taken from Lopaschuk, G. D., Karwi, Q. G., Tian, R., Wende, A. R., & Abel, E. D. (2021). Cardiac energy metabolism in heart failure. *Circulation research*, *128*(10), 1487-1513.

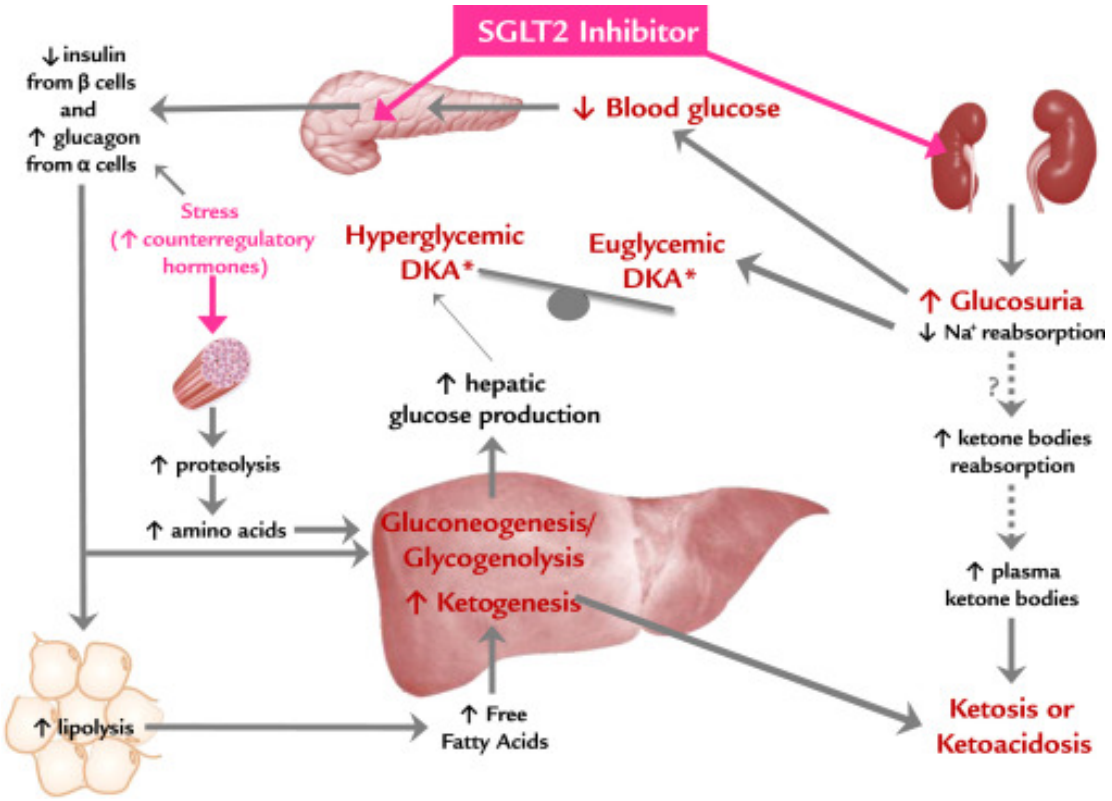

Figure 3. Action of sodium glucose co-transporter 2 inhibitors (SGLT2i). SGLT2i inhibit the proximal tubule in the kidney to prevent glucose reabsorption. Alongside increasing glycosuria, and natriuresis, SGLT2i also increase lipolysis and subsequent ketogenesis. Figure taken from Goldenberg, R. M., Berard, L. D., Cheng, A. Y., Gilbert, J. D., Verma, S., Woo, V. C., & Yale, J. F. (2016). SGLT2 inhibitor–associated diabetic ketoacidosis: clinical review and recommendations for prevention and diagnosis. *Clinical Therapeutics*, *38*(12), 2654-2664.

Chapter Two

RESEARCH METHODOLOGY

2.1 Experimental Animals

All protocols involving mice were approved by the University of Alberta Institutional Animal Care and Use Committee. All animals received treatment and care abiding to the guidelines of the Canadian Council on Animal Care, and all procedures on animals were approved by the University of Alberta Health Sciences Animal Welfare Committee. Male 7-week old adult C57BL/6N mice were obtained from Charles River Laboratories (Charles River, Quebec, Canada) and were used in this study. All mice were housed in a controlled environment in the University of Alberta Health Sciences Laboratory Animal Services (HSLAS) with temperature regulation alongside a 12-hour light and dark cycle. Mice had access to water and regular chow diet *ad libitum*. After acclimatizing to their new environment for 1 week, the now 8-week old mice were randomized to a sham surgery or a transverse aortic constriction (TAC) surgery to induce pressure overload hypertrophy over a 3-week period. After developing heart failure or not over the 3 weeks, cardiac function was assessed using echocardiography, and mice were further randomized to receive dapagliflozin or vehicle treatment for an additional 4 weeks. This divided the mice into 4 experimental groups: Sham Vehicle (n=10; Sham Veh), Sham Dapagliflozin (n = 11; Sham DAPA), TAC Vehicle (n= 13; TAC Veh), and TAC Dapagliflozin (n= 12; TAC DAPA). Following these 7 weeks, mice were euthanized and ex-vivo isolated working heart perfusions were conducted. The surgeon, technician conducting echocardiography, and technician conducting isolated working heart perfusions were blinded. The randomization schedule was created in advance of all surgeries and only myself and Dr. Lopaschuk knew the schedule.

2.2 Transverse Aortic Constriction Surgery

Cardiac pressure overload hypertrophy was induced by carrying out a transverse aortic constriction surgery. 8-week old mice were anesthetized via intraperitoneal injection, with ketamine and xylazine (100mg/kg and 20 mg/kg, respectively), intubated and connected to a mouse ventilator (MiniVent, Harvard Apparatus, Holliston, MA, USA). Following midline

sternotomy to access the heart, the aorta was surgically constricted against a blunt 27-gauge needle tied with a 6-0 non-absorbable silk suture, after which the suture was tightened, needle was removed, and the chest was stitched closed. Mice subjected to sham surgery underwent the same procedure but without constricting the aorta.

2.3 Body Weight Measurement

Body weight was measured biweekly during each of the 7 weeks during the protocol. Each mouse was individually removed from its cage and placed on a weighing scale measuring the weight to a single decimal point, following which it was placed back in its cage. Body weight was also measured at a single time point following a 16-hour fast during the 7^{th} week of the protocol, the day prior to ex-vivo isolated working heart perfusions.

2.4 Transthoracic Echocardiography

Following 3 and 6 weeks of TAC or sham surgery, mice were anesthetized with 3% isofluorane prior to transthoracic echocardiography carried out with a Vevo 3100 high-resolution image system equipped with a 30-MHz transducer (MX201 and MX550, VisualSonics, Toronto, ON, Canada) to assess *in vivo* cardiac function and confirm pressure overload heart failure. Mice were anesthetized via a nose cone on an electrocardiogram table with limbs attached to electrodes through Sigma electrode gel (Parker Laboratories). Ultrasound images were taken by applying Aquasonic clear ultrasound gel (Parker Laboratories). M mode images were taken for % EF, % FS, IVS:d, IVS:s, LVID:d, LVID:s, LVPW:d, LVPW:s, LA, LVEDV, LVESV, LV mass, E, A, e', a', and IVRT (full form for each given in the list of abbreviations above). A noninvasive measurement of area under the curve (mmHg) in pulse wave Doppler-mode was used to measure the pressure gradient across the transverse aortic constriction site.

2.5 Dapagliflozin Treatment

Following echocardiography at 3 weeks, Sham and TAC mice were randomized to either vehicle or dapagliflozin in their drinking water, according to a pre-determined randomization schedule prior to echocardiography. The % ejection fraction was used as an indicator of heart failure development in the TAC mice; if the % ejection fraction was above 50%, that mouse was not included into the study. Dapagliflozin was purchased from Cayman Chemical, and administered

at a dose of 1 mg/kg body weight daily. Dapagliflozin dose in the water was adjusted to body weight over the entire 7-week experimental protocol. Mice receiving vehicle just received standard water with no drug mixed in. This divided the mice into 4 experimental groups: Sham vehicle (n=10; Sham Veh), Sham Dapagliflozin (n = 11; Sham DAPA), TAC vehicle (n= 13; TAC Veh), and TAC Dapagliflozin (n= 12; TAC DAPA). The water intake was measured daily, where the amount of water in each bottle at the end of each day was measured and divided by the amount of mice per cage to get a rough estimate of amount of water each mouse drank per day.

2.6 Plasma Substrate Measurements

Following randomization to treatment or vehicle groups, blood glucose and blood ketone measurements were taken biweekly from the mice tail vein. One measurement per week was taken at the start of the mice's light cycle at 8:30am, and the second measurement per week was taken at the end of the mice's light cycle at 6:30pm. Biweekly measurements were taken 2-3 days apart to allow mice time to recover. Mice were restrained and their tail tips were pinched to produce a drop of blood. A Contour Next blood glucose meter and a Freestyle Precision Neo blood ketone meter paired with Contour Next and Freestyle Precision B-Ketone test strips, respectively, were used to measure blood glucose and ketone levels in millimolar (mM). A single fasted blood glucose and blood ketone measurement was also taken during the 7^{th} week of the protocol, the day prior to the ex-vivo working heart perfusions.

2.7 Glucose Tolerance Test (GTT)

During the 6^{th} week of the protocol, the mice were subjected to a glucose tolerance test to measure the rate of glucose clearance over a 3-hour period. Mice were fasted for 12 hours, and 1 hour prior to the test, a glucose bolus was calculated according to mouse's body weight. A 45% concentration of glucose and a dose of 2 mg glucose per g body weight was used. Mice were injected with the bolus into the peritoneum cavity and a blood glucose measurement was taken. This was time 0. Blood glucose measurements were taken at 15, 30, 60, 90, 120, and 180 minutes following glucose injection, following which food was returned to the mice cages.

2.8 Ex-Vivo Isolated Working Heart Perfusions

At the end of the 7-week period, 15-week old mice were anesthetized with an intraperitoneal injection of sodium pentobarbital (60 mg/kg body weight) and hearts were extracted, cannulated, and retrogradely perfused ex-vivo with Krebs-Henseleit solution. Immediately after the heart was extracted from the chest cavity, blood was also drawn from the cavity using a 1 ml syringe into a 1.5 mL Eppendorf tube containing 60 uL EDTA to prevent clotting. The tubes containing blood and EDTA were centrifuged for 10 minutes at 2500g. The supernatant which contained plasma, was extracted into separately labelled tubes and stored in -80 degrees ° C. The liver and kidney were also extracted from the mouse body, and these organs were snap frozen with liquid nitrogen, wrapped in aluminum foil, and stored in -80 degrees ° C.

Perfusion conditions for the hearts were as follows: 5 mM glucose, 0.8 mM palmitate bound to 3% albumin, 100 uM/ml insulin, and 2 various BOHB concentrations. Hearts were perfused for 30 minutes at 0.2 mmol BOHB, after which an additional 0.4 mmol BOHB was added to the perfusate, and hearts were perfused for another 30 minutes at 0.6 mmol BOHB. Absolute metabolic rates of BOHB oxidation, palmitate oxidation, glucose oxidation, and glycolysis were measures using radiolabelled substrates and collecting the radioactively labelled products passing through the metabolic pathways, as described previously [80, 153]. Each heart was perfused with two radiolabelled substrates to measure two metabolic pathways simultaneously; glucose oxidation and glycolysis, and palmitate oxidation and BOHB oxidation were measured together. This resulted in half of the mice in each experimental group being perfused with each each set of radiolabelled substrates. In the first group, 5-^{3}H/U-^{14}C glucose was used to measure rates of glycolysis and glucose oxidation through the collection of ^{3}H2O produced in glycolysis and ^{14}CO2 produced in glucose oxidation. In the second group, 9,10-^{3}H palmitate and 3-^{14}CβOHB were used to measure fatty acid oxidation and βOHB oxidation through the collection of ^{3}H2O and ^{14}CO2 respectively. Hyamine and buffer samples were taken at 10-minute intervals to calculate absolute metabolic rates. Ex-vivo functional parameters of heart rate (HR), peak systolic pressure (PSP), developed pressure (DP), HR x PSP, HR x DP, cardiac output, aortic output, coronary flow, cardiac work, and oxygen consumption were also measured from the ex-vivo isolated working heart perfusions at 10 minute intervals. Cardiac efficiency was calculated as cardiac work divided by oxygen consumption.

State state rates of ATP production from exogenous substrates were calculated with the values of 2 and 30 mol ATP/mol of glucose passing through glycolysis and glucose oxidation, respectfully, 22 mol ATP/mol BOHB oxidized through BOHB oxidation, and 105 mol ATP/mol palmitate oxidized from palmitate oxidation**.** Rates of Acetyl-CoA production were calculated with the values of 2 mol Acetyl-CoA each produced from glucose oxidation and BOHB oxidation, and 8 mol Acetyl-CoA produced from palmitate oxidation.

2.9 Immunoblotting

Following isolated working heart perfusions, hearts were snap frozen in liquid Nitrogen. Mice livers were also extracted during this time and also snap frozen in liquid Nitrogen. All subsequent immunoblotting steps were done the same for each organ. Thirty to thirty-five milligrams of frozen tissue was homogenized for 60 seconds (2 x 30 second intervals) with a Polytron homogenizer in a buffer of pH 7.5 containing 50 mmol/L Tris-HCL, 150 mmol/L NaCl, 0.5% NP-40, 1% Triton-X 100, 5 mmol/L EDTA, and 0.1% SDS in the presence of phosphatase (1/ 100 total dilution) and protease inhibitors (1/100 total dilution) (MilliporeSigma), as well as deacetylase inhibitors (10 mmol/L nicotinamide, 10 umol/l trichostatin A, and 10mmol/L sodium butyrate). Thirty micrograms of the denatured proteins was subjected to 10% SDS-PAGE and 30 micrograms of protein was loaded into each well; the gels were run at 80 volts for 30 minutes and 120 volts for approximately 90 minutes. A ladder (Bio-Rad Precision Plus Protein Duel Color Standards) was used to represent approximate molecular weights on the gel. The gels were transferred to nitrocellulose membranes overnight at approximately 22 volts. After blocking in 5% fat-free milk for 2.5 hours, membranes were probed with one of the following primary antibodies for 1 hour at room temperature or overnight incubation in 4° C: SCOT (1: 1000, Proteintech, 12175-1AP), BDH-1 (1: 5000, Novus Bioceuticals, NBPI-88673), NALP3 (1: 1000 dilution, Epitomics 3560-1). Membranes were washed for 30 minutes with 1x TBST (tris-buffered saline buffer with Tween 20), then incubated with the appropriate secondary antibodies (goat anti-rabbit, Biorad Laboratiores Inc. 170-6515 ; goat anti-mouse, Biorad Laboratories Inc. 170-6516) at a 1:5000 dilution for 1 hour at room temperature Membranes were washed again for 30 minutes with 1X TBST. Bands were visualised with enhanced chemiluminescence on FUJU X-ray film in a Protec OPTIMAX-X-ray Film Processor, and quantified with ImageJ

software (NIH). Tubulin (1: 10,000, Sigma-Aldrich T6074) was used as an internal loading control to normalize for any variation in protein loading between samples.

2.10 Statistical Analysis

Data are represented as means +/- SEM or means +/- SD. Comparisons and significant differences between experimental groups were determined by using a one-way ANOVA followed by Sidak's post-hoc test. The correlation was examined by linear regression analysis using the least-squares method. Statistical analysis was carried out using commercially available software (GraphPad Prism V8). A p value < 0.05 was considered statistically significant.

Chapter Three

RESULTS

3.1. Dapagliflozin improves body weight in sham mice, and does not affect insulin sensitivity

Of the 46 mice that underwent TAC or sham surgery and reached the final endpoint of perfusions, there were 10 mice in the Sham Veh group, 11 mice in the Sham DAPA group, 13 mice in the TAC Veh group, and 12 mice in the TAC DAPA group. Following TAC and sham surgeries, we measured the body weight of the mice biweekly over the entire 7-week protocol to determine whether dapagliflozin treatment has an effect on body weight. We observed a significant decrease in body weight in the Sham DAPA group compared to the Sham Veh group over 7 weeks, confirming the function of SGLT2i in promoting glycosuria and naturiesis (**Figure 1A).** However, a significant decrease in body weight was not seen in the TAC DAPA group compared to TAC Vehicle, nor were there any significant differences in body weight observed between the Sham Veh and TAC Veh, and Sham DAPA and TAC DAPA groups (i.e. with TAC) (**Figure 1A).** Following a 16-hour fast, the body weight was not significantly different between the experimental groups; however, there was a trend towards lower body weight at this time-point in the groups treated with dapagliflozin relative to their respective controls (**Figure 1B)**. A glucose tolerance test was conducted during the third week of treatment. There were no significant differences in glucose clearance observed between the groups over the 3 hour-time point (**Figure 1C)**; however, the area under the curve was significantly lower for the TAC Veh group compared to Sham Veh (**Figure 1D)**.

3.2 Dapagliflozin does not significantly improve blood ketone and glucose levels during the light cycle and following a 16-hour fast.

Circulating ketone and glucose levels were measured biweekly through the entire 4-week treatment protocol to assess the effect of dapagliflozin and determine the in-vivo circulating levels of those substrates with their respective treatment. Ketone levels at the beginning and end of the light cycle showed no significant differences between experimental groups (**Figure 2A-B).** 16-hour fasted ketone levels also did not show any significant differences between groups; however, there was a trend towards increased circulating ketones in the fasted state in the Sham

DAPA and TAC DAPA groups compared to their respective controls **(Figure 2C)**. Glucose levels at the beginning and end of the light cycle, as well as levels following a 16-hour fast showed no significant differences between groups **(Figure 2 D-F)**.

3.3 Dapagliflozin has no improvement on cardiac function

Echocardiography was performed at 3 weeks post TAC or sham surgery to assess in vivo cardiac function, after which the hearts subjected to TAC had developed pressure-overload hypertrophy HF over 3 weeks. This was done prior to dapagliflozin treatment, and referred to as the baseline, pre-treatment, or 3-week echo assessment; therefore, Sham and DAPA groups are identical here (the names represent the groups the hearts were randomized into following the echo assessment). Baseline echocardiography results confirmed the establishment of pressure-overload hypertrophy and HF in TAC mice, as shown by a reduction in markers of systolic function: % ejection fraction (33.60 ± 8.9 % in TAC Veh vs 55.14 ± 2.8% in Sham Veh; 37.31 ± 8.4 % in TAC DAPA vs 54.95 ± 7.8 % Sham DAPA) and % fractional shortening (15.93 ± 4.7 % in TAC Veh vs 28.27 ± 1.8 % in Sham Veh; 17.88 ± 4.6 % in TAC DAPA vs 28.34 ± 5.3 % Sham DAPA) in TAC mice compared to their sham controls (**Figure 3A-B and Table 1)**. Markers of hypertrophy: left ventricle posterior wall thickness at diastole (0.83 ± 0.15 mm in TAC Veh vs 0.6 ± 0.007 mm in Sham Veh; 0.76 ± 0.11 mm in TAC DAPA vs 0.57 ± 0.007 mm in Sham DAPA) and intraventricular septum wall thickness at diastole (0.81 ± 0.14 mm in TAC Veh vs 0.60 ± 0.06 mm in Sham Veh; 0.74 ± 0.13 mm in TAC DAPA vs. 0.54 ± 0.07 mm in Sham DAPA) were also increased in TAC mice compared to their sham controls **(Table 1)**. Diastolic dysfunction, namely E/E', was significantly worse in TAC mice (-41.39 ± 16.95 in TAC Veh vs. -23.74 ± 3.06 in Sham Veh), while E/A ratio, isovolumic relaxation time, and left atrium size did not vary significantly between any of the groups at 3 weeks post-TAC **(Figure 3C and Table 1).**

Within one day following the echocardiography assessment at 3 weeks, mice were randomized to receive either dapagliflozin in their drinking water at a dose of 1 mg/kg/bw, or standard drinking water (Veh). 3 weeks later, echocardiography was done again to assess in vivo cardiac function following 3 weeks of treatment with dapagliflozin; this is referred to the post-treatment or 6-week echocardiography assessment. The same trends observed at 3 weeks persisted, with % ejection fraction (27.71 ± 10.0 % in TAC Veh vs 54.46 ± 3.7 % in Sham Veh; 31.94 ± 9.9 % in

TAC DAPA vs 54.33 ± 3.7 % in Sham DAPA) and % fractional shortening (12.99 ± 4.9 % in TAC Veh vs 27.94 ± 2.3 % in Sham Veh; 15.12 ± 5.0 % in TAC DAPA vs 27.78 ± 2.4 % in Sham DAPA) significantly decreased in TAC groups compared to their respective sham groups, and left ventricle posterior wall thickness at diastole (0.82 ± 0.18 mm in TAC Veh vs 0.58 ± 0.05 mm in Sham Veh; 0.76 ± 0.11 mm in TAC DAPA vs 0.58 ± 0.06 mm in Sham DAPA) and interventricular septum wall thickness at diastole (0.81 ± 0.14 mm in TAC Veh vs 0.60 ± 0.09 mm in Sham Veh; 0.75 ± 0.12 mm in TAC DAPA vs 0.58 ± 0.05 mm in Sham DAPA) significantly higher in TAC groups compared to their respective controls **(Figure 3 A, B, and Table 1).** Additionally, left ventricle mass (125.86 ± 49.6 mg in TAC Veh vs 69.22 ± 15.7 mg in Sham Veh; 107.59 ± 41.9 mg in TAC DAPA vs 62.87 ± 9.6 mg in Sham DAPA), left ventricle internal diameter at systole (4.12 ± 0.7 mm in TAC Veh vs 2.97 ± 0.3 mm in Sham Veh; 3.80 ± 0.8 mm in TAC DAPA vs 2.91 ± 0.3 mm in Sham DAPA), left ventricle end systolic volume (75.96 ± 33.6 ul in TAC Veh vs 36.04 ± 7.4 ul in Sham Veh; 64.55 ± 33.3 ul in TAC DAPA vs 32.82 ± 6.2 ul in Sham DAPA), and E/E' (-48.47 ± 17.76 in TAC DAPA vs -26.67 ± 4.73 in Sham DAPA) was also significantly increased in TAC mice **(Figure 3C, D and Table 1)**. However, these significant changes were only seen between TAC groups and their respective controls; and there was no improvement observed in any of the cardiac function parameters with dapagliflozin treatment.

3.4 Dapagliflozin does not significantly affect substrate metabolic rates

Rates of glycolysis and glucose, BOHB, and palmitate oxidation were measured in ex-vivo isolated working heart perfusions at 2 concentrations of BOHB: 0.2 mM BOHB and 0.6 mM BOHB, to represent normal circulating BOHB levels (lower concentration) and BOHB levels seen in the blood with dapagliflozin treatment (higher concentration). These values were determined from both ketone levels measured in vivo with dapagliflozin treatment, and from our previous study [80]. Glucose oxidation showed no significant differences with dapagliflozin treatment at either 0.2 mM or 0.6 mM ketones (**Figure 4A)**. However, there was a trend towards higher glucose oxidation rates in the TAC DAPA group compared to TAC Veh at both BOHB concentrations (**Figure 4A)**. Additionally, our results also showed that glucose oxidation rates are lower in the failing heart (532.8 ± 99.0 nmol • g dry wt^{-1} • min^{-1} in TAC veh vs 1352 ± 221.7 nmol • g dry wt^{-1} • min^{-1} in Sham Veh at 0.2 mM BOHB), confirming our previous studies [80],

and that increasing the concentration of BOHB in the perfusate does not further impair glucose oxidative rates in the failing heart (838.6 ± 147.1 nmol • g dry wt^{-1} • min^{-1} in TAC veh at 0.6 mM BOHB vs 532.8 ± 99.0 nmol • g dry wt^{-1} • min^{-1} in TAC Veh at 0.2 mM BOHB) **(Figure 4A).** When normalized per unit work, there were no significant differences observed between groups at both BOHB concentrations **(Figure 5A).**

Glycolytic rates showed no changes with dapagliflozin treatment, as there were no significant differences in glycolytic rates between groups (**Figure 4B)**. When normalized per unit work, there were no significant differences observed between groups; however, there was a trend towards increased glycolytic rates in both TAC groups compared to their Sham controls at 0.2 mM BOHB, especially in TAC Veh, supporting our previous findings and providing further evidence that the failing heart relies more on glycolysis for ATP production [34] (**Figure 5B).**

BOHB oxidation rates showed no significant differences between groups both 0.2 mM and 0.6 mM BOHB; however, there was a trend towards increased BOHB oxidation at 0.6 mM BOHB in both DAPA groups compared to their respective controls **(Figure 4C)**. Additionally, BOHB oxidation increased significantly at around a 3-fold increase at 0.6 mM BOHB for each experimental group (92.80 ± 12.04 nmol • g dry wt^{-1} • min^{-1} vs 31.33 ± 5.16 nmol • g dry wt^{-1} • min^{-1} in Sham Veh; 118.0 ± 9.02 nmol • g dry wt^{-1} • min^{-1} vs 37.0 ± 2.38 nmol • g dry wt^{-1} • min^{-1} in Sham DAPA; 78.0 ± 10.58 nmol • g dry wt^{-1} • min^{-1} vs 24.33 ± 5.89 nmol • g dry wt^{-1} • min^{-1} in TAC Veh; 114.1 ± 22.61 nmol • g dry wt^{-1} • min^{-1} vs 32.0 ± 4.1 nmol • g dry wt^{-1} • min^{-1} in TAC DAPA**)** (**Figure 4C)**. When normalized per unit work, we observed a trend towards higher BOHB rates in both TAC groups at both 0.2 mM BOHB and 0.6 mM BOHB, and this was significant in the TAC Veh group compared to Sham Veh at 0.6 mM BOHB (99.83 ± 26.29 nmol • Joules in TAC Veh vs 37.50 ± 2.77 nmol • Joules in Sham Veh) **(Figure 5C).** Additionally, we also observed that both TAC Veh and TAC DAPA groups had significantly increased BOHB rates per unit work at 0.6 mM BOHB compared to 0.2 mM BOHB (99.83 ± 26.29 nmol • Joules in TAC Veh at 0.6 mM BOHB vs 40.66 ± 12.81 nmol • Joules at 0.2 mM BOHB; 91.93 ± 13.36 nmol • Joules in TAC DAPA at 0.6 mM BOHB vs 34.15 ± 6.61 nmol • Joules at 0.2 mM) **(Figure 5C).**

Palmitate oxidation showed no significant differences with dapagliflozin treatment at both 0.2 mM BOHB and 0.6 mM BOHB; however, there was a trend towards lower palmitate oxidation rates in all experimental groups at 0.6 mM BOHB compared to 0.2 mM BOHB (**Figure 4D).** This was statistically significant in the TAC DAPA group (162.3 ± 22.30 nmol • g dry wt^{-1} • min^{-1} at 0.6 mM BOHB vs 355.8 ± 58.6 nmol • g dry wt^{-1} • min^{-1} at 0.2 mM) **(Figure 4D).** When normalized per unit work, palmitate oxidation rates were significantly increased in both TAC groups compared to their respective controls at 0.2 mM BOHB (382.2 ± 90.7 nmol • Joules in TAC Veh vs 114.3 ± 21.0 nmol • Joules in Sham Veh; 375.4 ± 69.4 nmol • Joules in TAC DAPA vs 94.0 ± 27.7 nmol • Joules in Sham DAPA), although there was no significant difference with dapagliflozin (**Figure 5D)**. This trend was still present at 0.6 mM BOHB; however, it was not significant, and here also dapagliflozin had no effect on palmitate oxidation rates (**Figure 5D).**

3.5 Dapagliflozin does not improve cardiac work or O2 consumption

Both TAC Veh and TAC Dapa groups had significantly lower cardiac work compared to their sham controls throughout the entire 60-minute perfusion (**Figure 6A)**. Dapagliflozin had no significant improvement in cardiac work between groups. Oxygen consumption **(Figure 6B)** and cardiac output (**Figure 6C)** showed the same results as cardiac work, as both were lower in both TAC groups with no significant improvement with dapagliflozin treatment. Table 2 shows each ex-vivo cardiac function parameter at 0.2 mM BOHB and 0.6 mM BOHB.

3.6 Dapagliflozin improves Acetyl-CoA and ATP production in TAC hearts

We observed both TAC groups to have lower acetyl-CoA production compared to their Sham controls at 0.2 mM, but this was not significant **(Figure 7A)**. However, both TAC groups, did have significantly lower acetyl-CoA production compared to their Sham controls at 0.6 mM BOHB (3.14 umol • g dry wt^{-1} • min^{-1} in TAC Veh vs 4.79 umol • g dry wt^{-1} • min^{-1} in Sham Veh; 4.03 umol • g dry wt^{-1} • min^{-1} in TAC DAPA vs 5.75 umol • g dry wt^{-1} • min^{-1} in Sham DAPA) **(Figure 7A).** Although dapagliflozin did not show any significant differences in acetyl-CoA production at both 0.2 mM BOHB and 0.6 mM BOHB, we did observe a trend towards increased acetyl-CoA production in both DAPA groups compared to their controls at both BOHB concentrations, this was more apparent in TAC DAPA compared to TAC Veh (**Figure 7A)**. When the contribution of each substrate oxidation to total acetyl-CoA production was graphed,

we observed that a greater proportion of acetyl-CoA was produced from palmitate oxidation in both TAC groups compared to their Sham controls at 0.2mM BOHB (66.9 % in TAC Veh vs 39.7 % in Sham Veh; 60.9% in TAC DAPA vs 38.4 % in Sham DAPA**),** resulting in a lower contribution of glucose oxidation (31.6 % in TAC Veh vs 58.9 % in Sham Veh; 37.7 % in TAC DAPA vs 60.2 % in Sham DAPA) **(Figure 7B).** At 0.6 mM BOHB, the contribution of palmitate oxidation to acetyl-CoA in both TAC groups was slightly less than at 0.2 mM BOHB (41.6% in TAC Veh 0.6 mM BOHB vs 66.9% at 0.2 mM BOHB; 32.2% in TAC DAPA 0.6 mM BOHB vs 60.9% at 0.2 mM BOHB) **(Figure 7B),** consistent with lower absolute palmitate oxidation rates (**Figure 4D)** and palmitate rates normalized to cardiac work in both TAC groups at 0.6 mM **(Figure 5D).** BOHB oxidation contributed a greater proportion of acetyl-CoA in each group at 0.6 mM BOHB compared to 0.2 mM BOHB (3.9% vs 1.37% in Sham Veh; 4.1% vs 1.4 % in Sham DAPA; 5.0% vs 1.44% in TAC Veh; 5.68% vs 1.37% in TAC DAPA) **(Figure 7B).** The greatest contribution of acetyl-CoA came from glucose oxidation and palmitate oxidation.

Total ATP production was significantly lower in the TAC Veh group compared to the Sham Veh group at both 0.2 mM BOHB and 0.6 mM BOHH (71.39 umol • g dry wt^{-1} • min^{-1} in TAC Veh vs 87.84 umol • g dry wt^{-1} • min^{-1} in Sham Veh at 0.2 mM BOHB; 65.09 umol • g dry wt^{-1} • min^{-1} in TAC Veh vs 106.49 umol • g dry wt^{-1} • min^{-1} in Sham Veh at 0.6 mM BOHB) , and significantly lower in the TAC DAPA group compared to the Sham DAPA group at 0.6 mM BOHB (92.41 umol • g dry wt^{-1} • min^{-1} in TAC DAPA vs 111.52 umol • g dry wt^{-1} • min^{-1} in Sham DAPA); there was a slight downwards trend in the TAC DAPA group compared to Sham DAPA at 0.2 mM BOHB, but it was not significantly lower (**Figure 7C).** Dapagliflozin significantly improved total ATP production in the TAC DAPA group compared to TAC Veh groups at both 0.2 mM and 0.6 mM BOHB (93.16 umol • g dry wt^{-1} • min^{-1} in TAC DAPA vs 71.39 umol • g dry wt^{-1} • min^{-1} in TAC Veh at 0.2 mM BOHB; 92.42 umol • g dry wt^{-1} • min^{-1} in TAC DAPA vs 65.1 umol • g dry wt^{-1} • min^{-1} in TAC Veh at 0.6 mM BOHB) (**Figure 7C).** Additionally, increasing the concentration of BOHB in the perfusate resulted in a significant increase in total ATP production in the Sham Veh group (106.49 umol • g dry wt^{-1} • min^{-1} vs 87.84 umol • g dry wt^{-1} • min^{-1}), while not affecting any of the other three groups **(Figure 7C).** When the contribution of each substrate oxidation to total ATP production was graphed, the same trends were observed as in the graph showing the contribution of each substrate oxidation to total acetyl-CoA production. A greater

proportion of ATP was produced from palmitate oxidation in both TAC groups compared to their Sham controls at 0.2mM BOHB (41.4 % in TAC Veh vs 27.2 % in Sham Veh; 40.1% in TAC DAPA vs 26.4 % in Sham DAPA**),** resulting in a lower contribution of glucose oxidation (22.4 % in TAC Veh vs 46.2 % in Sham Veh; 28.3 % in TAC DAPA vs 47.4 % in Sham DAPA) **(Figure 7D).** At 0.6 mM BOHB, the contribution of palmitate oxidation to ATP in both TAC groups was slightly less than at 0.2 mM BOHB (26.37% in TAC Veh 0.6 mM BOHB vs 41.4% at 0.2 mM BOHB; 18.4% in TAC DAPA 0.6 mM BOHB vs 40.1% at 0.2 mM BOHB) **(Figure 7D),** consistent with lower absolute palmitate oxidation rates (**Figure 4D)** and palmitate rates normalized to cardiac work in both TAC groups at 0.6 mM **(Figure 5D).** BOHB oxidation contributed a greater proportion of ATP in each group at 0.6 mM BOHB compared to 0.2 mM BOHB (1.9% vs 0.78% in Sham Veh; 2.3% vs 0.81 % in Sham DAPA; 2.6% vs 0.75% in TAC Veh; 2.7% vs 0.76% in TAC DAPA) **(Figure 7D).** The greatest contribution of ATP came from glycolysis, glucose oxidation, and palmitate oxidation.

3.7 Dapagliflozin increases cardiac efficiency when perfused with higher ketones

Cardiac efficiency over the first 30 minutes of the perfusion at 0.2 mM BOHB showed that TAC Veh hearts were significantly less efficient than Sham Veh hearts **(Figure 8A).** Cardiac efficiency over the second half of the perfusion at 0.6 mM BOHB showed both TAC Veh and TAC Dapa hearts were significantly less efficient than their Sham controls **(Figure 8A)**. However, we also observed that with 0.6 mM BOHB in the perfusate, TAC DAPA hearts had a significantly higher cardiac efficiency compared to TAC Veh hearts (**Figure 8A).**

Cardiac work normalized to Acetyl-CoA production is another measure of cardiac efficiency. We observed a significant decrease in both TAC groups compared to their Sham controls at both BOHB concentrations **(Figure 8B).** Additionally, we also observed a trend towards increased values in the TAC Dapa group compared to the TAC Veh group at both 0.2 mM BOHB and 0.6 mM BOHB **(Figure 8B)**, consistent with the significant increase in the cardiac efficiency measured during ex vivo isolated working heart perfusions at 0.6 mM BOHB in TAC DAPA compared to TAC Veh (**Figure 8A).**

3.8 Dapagliflozin decreases protein expression of SCOT in sham hearts with no significant effect on BDH-1 protein expression

Due to the increase in absolute BOHB oxidation rates and BOHB rates per unit work with increased ketones in the perfusate, we decided to assess the expression of oxidative enzymes involved in the BOHB oxidation pathway. Although there was no significance, BDH-1 expression levels showed a very high trend towards increased expression in TAC Veh out of all groups (**Figure 9A)**. Additionally, both TAC Veh and TAC DAPA groups showed trends for higher BDH-1 expression compared to their Sham controls, although this was not significant. (**Figure 9A).** There were no significant differences observed with DAPA treatment; however, there was a trend towards lower BDH-1 expression in the TAC DAPA group compared to TAC Veh (**Figure 9A)**. Protein expression of SCOT, the rate limiting enzyme of BOHB oxidation, showed a significant decrease in Sham DAPA compared to Sham Veh, as well as in TAC Veh compared to Sham Veh **(Figure 9B).** There was no significant difference observed in TAC DAPA compared to TAC Veh **(Figure 9B)**.

3.9 Dapagliflozin decreases Protein Expression of NRLP3/NALP3 Inflammasome

SGLT2i have also been proposed to exert their cardioprotective effects in the failing heart through modulating inflammation through the nod-like receptor family protein 3 inflammasome (NLRP3/NALP3) inflammatory pathway (NALP3 is another name for NLRP3). Therefore, we decided to assess the protein expression of the NRLP3/NALP3 inflammasome. Although there was no significance between any of the groups, we observed a trend towards decreased NALP3 protein expression in both DAPA groups compared to their respective controls **(Figure 10A).**

3.10 Figures and Tables

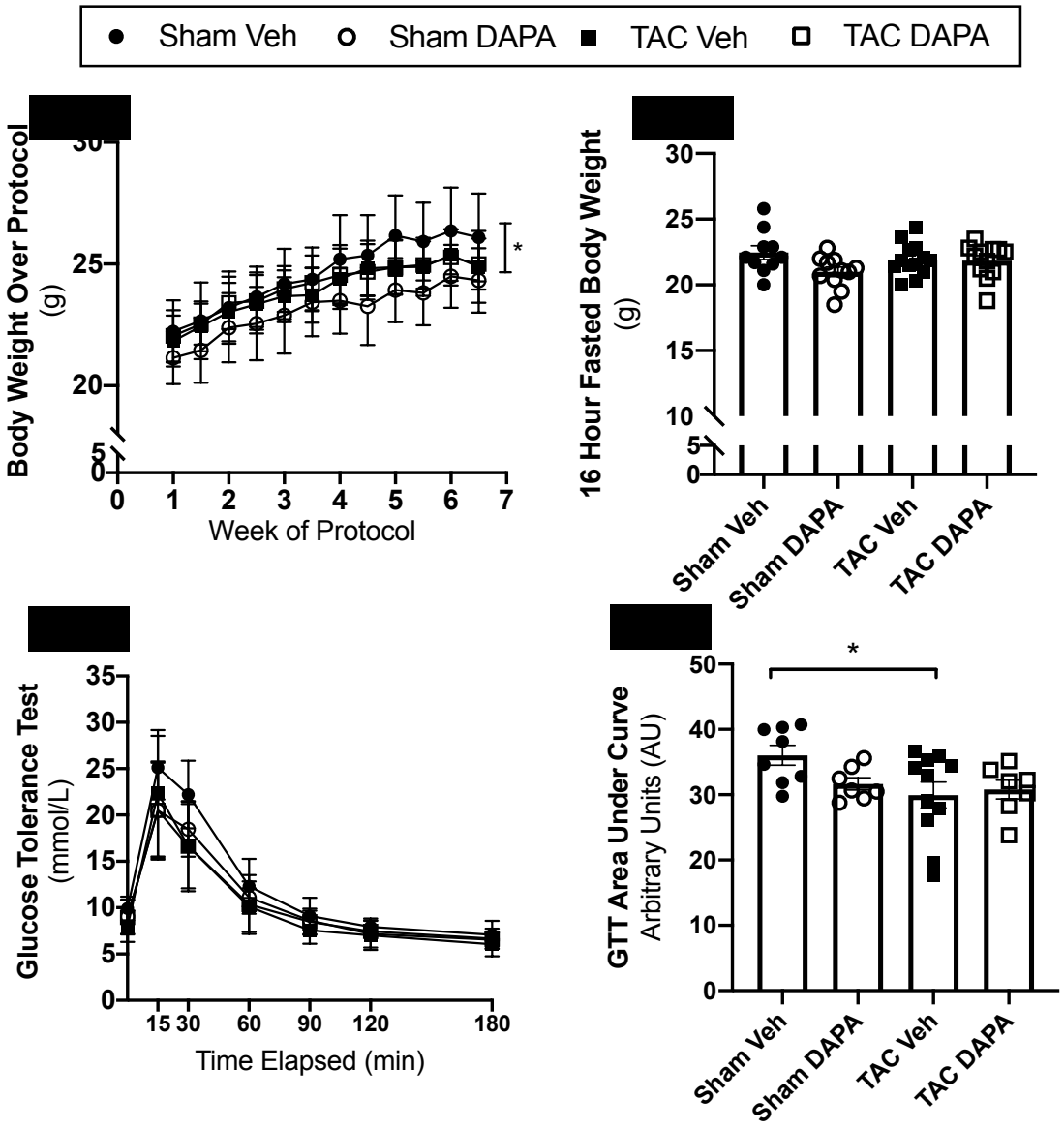

Figure 1. Dapagliflozin Treatment Parameters: Body Weight and Glucose Tolerance Test in Sham and TAC Mice Treated with Either Vehicle or Dapagliflozin. *(A)* Body weight over entire 7-week treatment protocol (n = 10-13). *(B)* Body weight following a 16-hour fast at the end of the 7-week protocol (n=10-13). *(C)* Glucose tolerance test (GTT) glucose levels (n=10-13). *(D)* Area under the curve for GTT (n = 10-13). Data are presented as means ± SD for A and C; means ± SEM for B and D. Data was analyzed by One-Way ANOVA followed by Sidak's multiple-comparison test. $^{*}P < 0.05$. DAPA, Dapagliflozin; Veh, Vehicle.

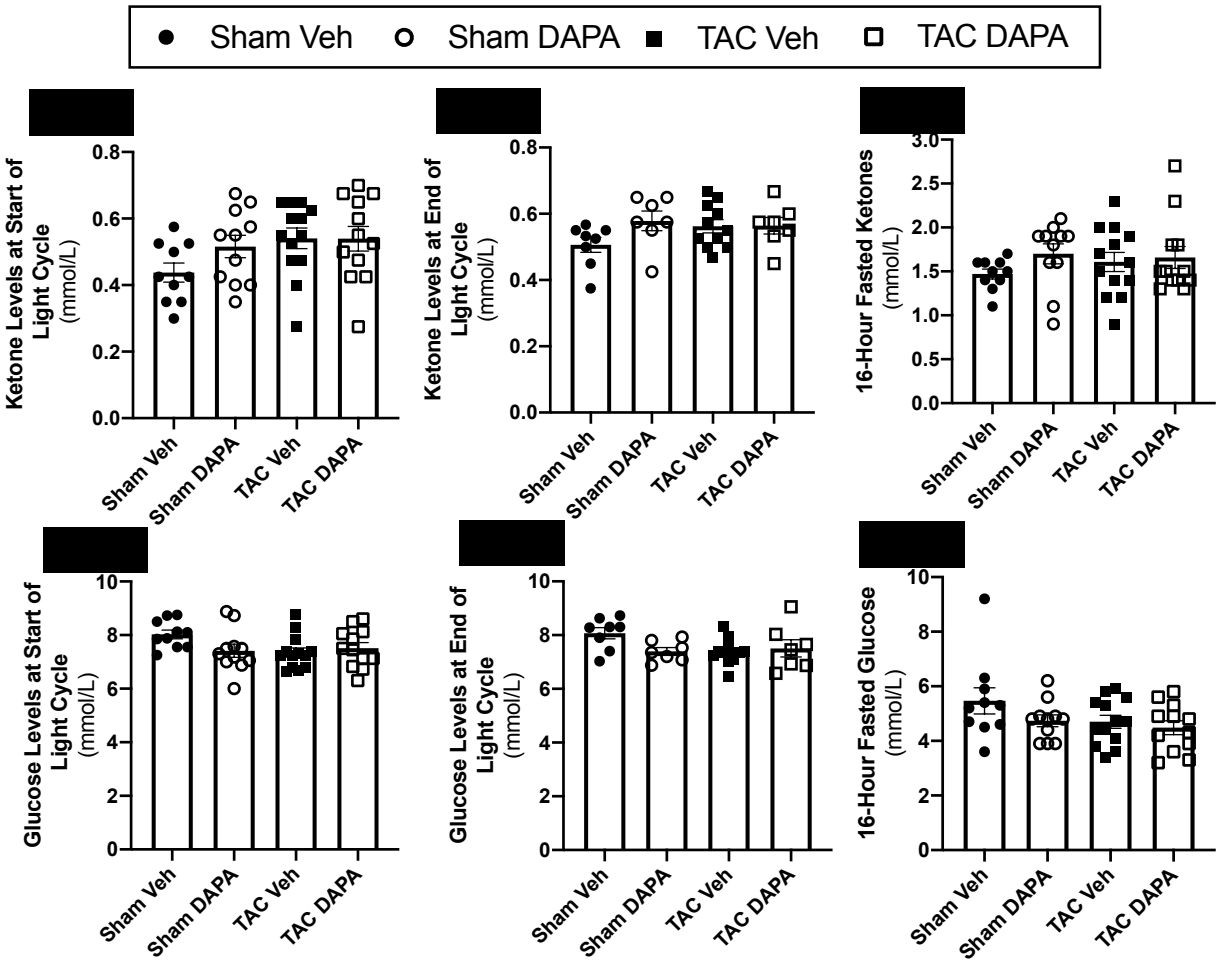

Figure 2. Ketone and Glucose Levels Taken Either Biweekly During Treatment Period or Following a 16-Hour Fast at the End of the Protocol in Sham and TAC Mice Treated with Either Vehicle or Dapagliflozin. *(A)* Ketone levels at the start of the light cycle (n = 10-13). *(B)* Ketone levels at the end of light cycle (n=10-13). *(C)* Ketone levels following a 16-hour fast at the end of the 7-week protocol (n=10-13). *(D)* Glucose levels at the start of the light cycle (n = 10-13). *(E)* Glucose levels at the end of light cycle (n=10-13). *(F)* Glucose levels following a 16-hour fast at the end of the 7-week protocol (n=10-13). Data are presented as means ± SEM. Data was analyzed by One-Way ANOVA followed by Sidak's multiple-comparison test. $^{*}P < 0.05$. DAPA, Dapagliflozin; Veh, Vehicle.

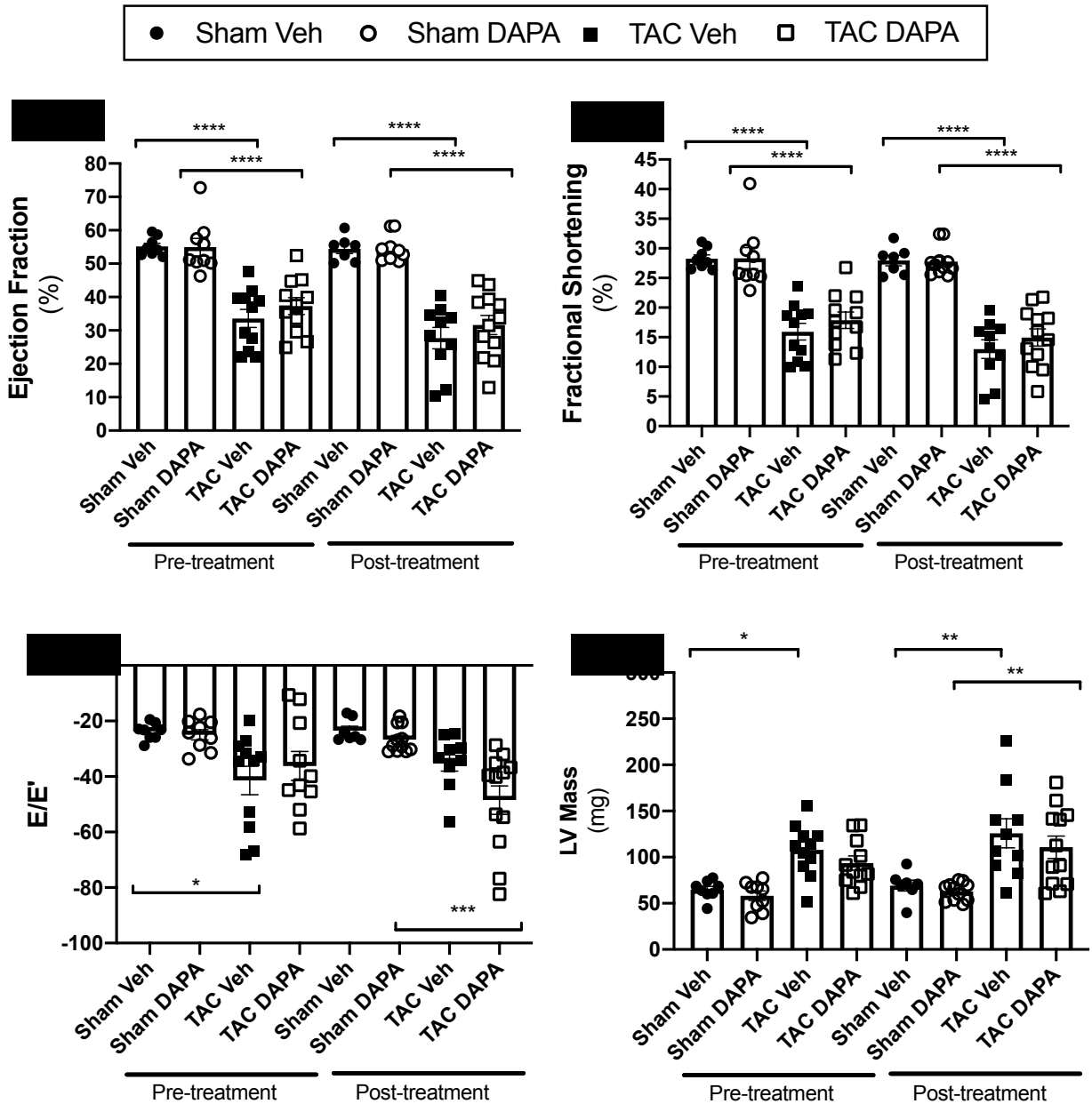

Figure 3. Cardiac Function in Sham and TAC Mice Treated with Either Vehicle or Dapagliflozin. *(A)* % Ejection fraction (n = 10-13). *(B)* % Fractional shortening (n=10-13). *(C)* E/E' (n=10-13). *(D)* LV mass (n = 10-13). Data are presented as means ± SEM. Data was analyzed by One-Way ANOVA followed by Sidak's multiple-comparison test. $^{*}P < 0.05$, $^{**}P < 0.005$, $^{***}P < 0.0005$, $^{****}P < 0.0001$. DAPA, Dapagliflozin; Veh, Vehicle.

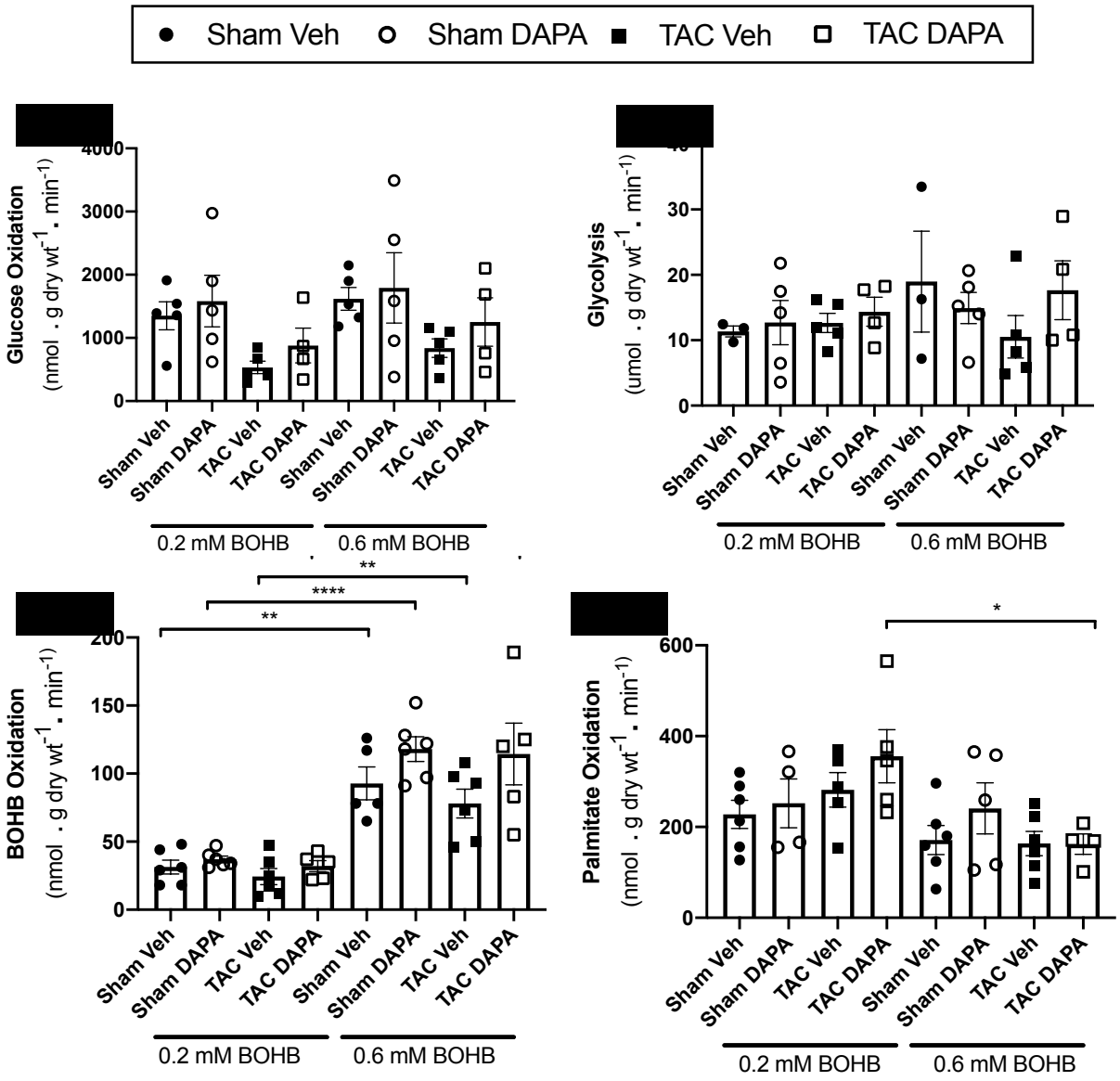

Figure 4. Absolute Oxidation Rates at 0.2 mM BOHB and 0.6 mM BOHB in Sham and TAC Mice Treated with Either Vehicle or Dapagliflozin. Metabolic rates are shown for *(A)* Glucose Oxidation (n = 5-6), *(B)* Glycolysis (n=3-5), *(C)* Betahydroxybutyrate (BOHB) Oxidation (5-6), and *(D)* Palmitate Oxidation (n = 5-6). Data are presented as means ± SEM. Data was analyzed by One-Way ANOVA followed by Sidak's multiple-comparison test. $^{*}P < 0.05$, $^{**}P < 0.005$, $^{***}P < 0.0005$, $^{****}P < 0.0001$. DAPA, Dapagliflozin; Veh, Vehicle.

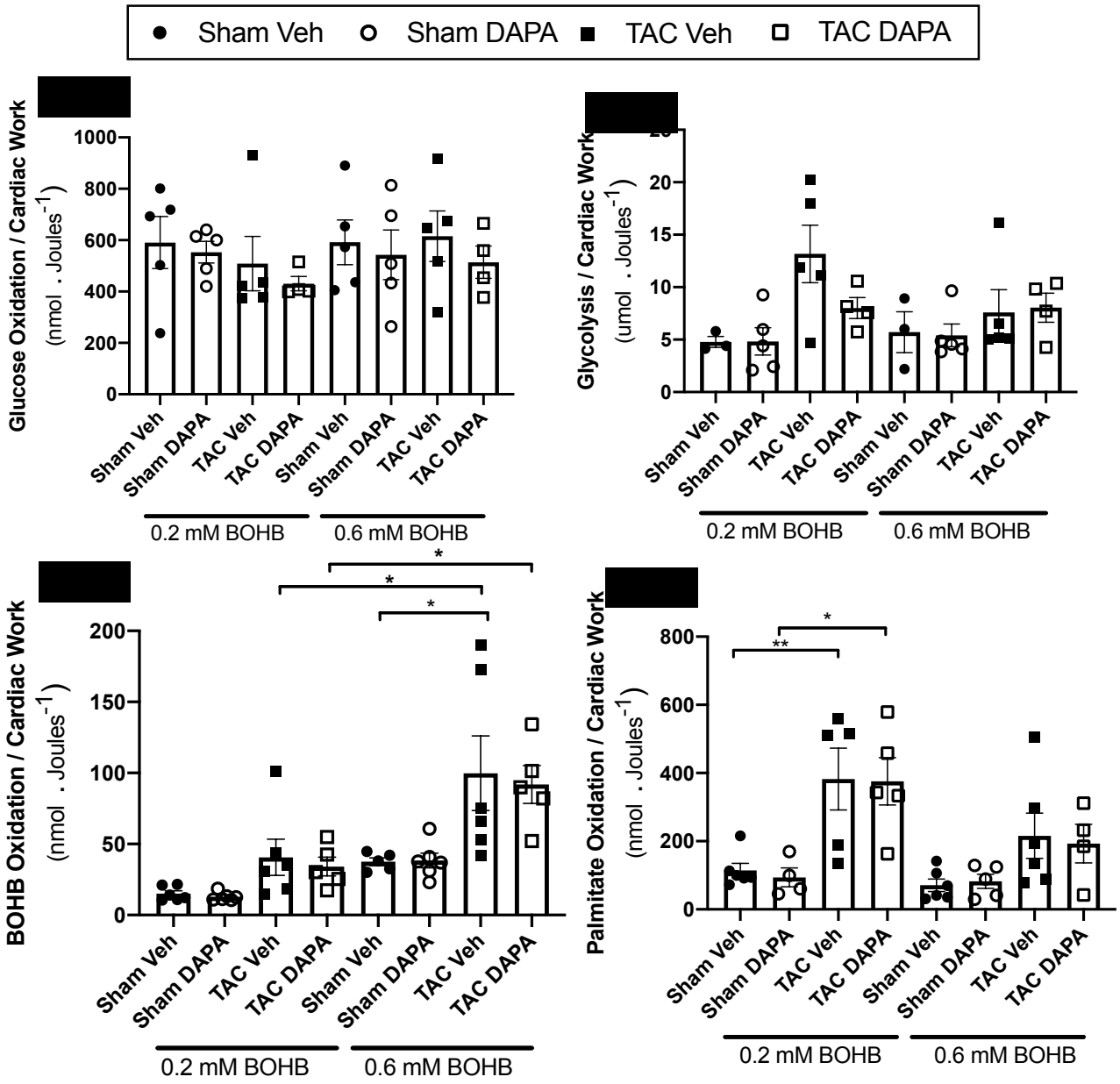

Figure 5. Oxidation Rates Normalized to Cardiac Work at 0.2 mM BOHB and 0.6 mM BOHB in Sham and TAC Mice Treated with Either Vehicle or Dapagliflozin. Metabolic rates are shown for *(A)* Glucose Oxidation normalized to cardiac work (CW) (n = 5-6), *(B)* Glycolysis normalized to cardiac work (CW) (n=3-5), *(C)* BOHB Oxidation normalized to cardiac work (CW) (5-6), and *(D)* Palmitate Oxidation normalized to cardiac work (CW) (n = 5-6). Data are presented as means ± SEM. Data was analyzed by One-Way ANOVA followed by Sidak's multiple-comparison test. $^{*}P < 0.05$, $^{**}P < 0.005$, $^{***}P < 0.0005$, $^{****}P < 0.0001$. DAPA, Dapagliflozin; Veh, Vehicle.

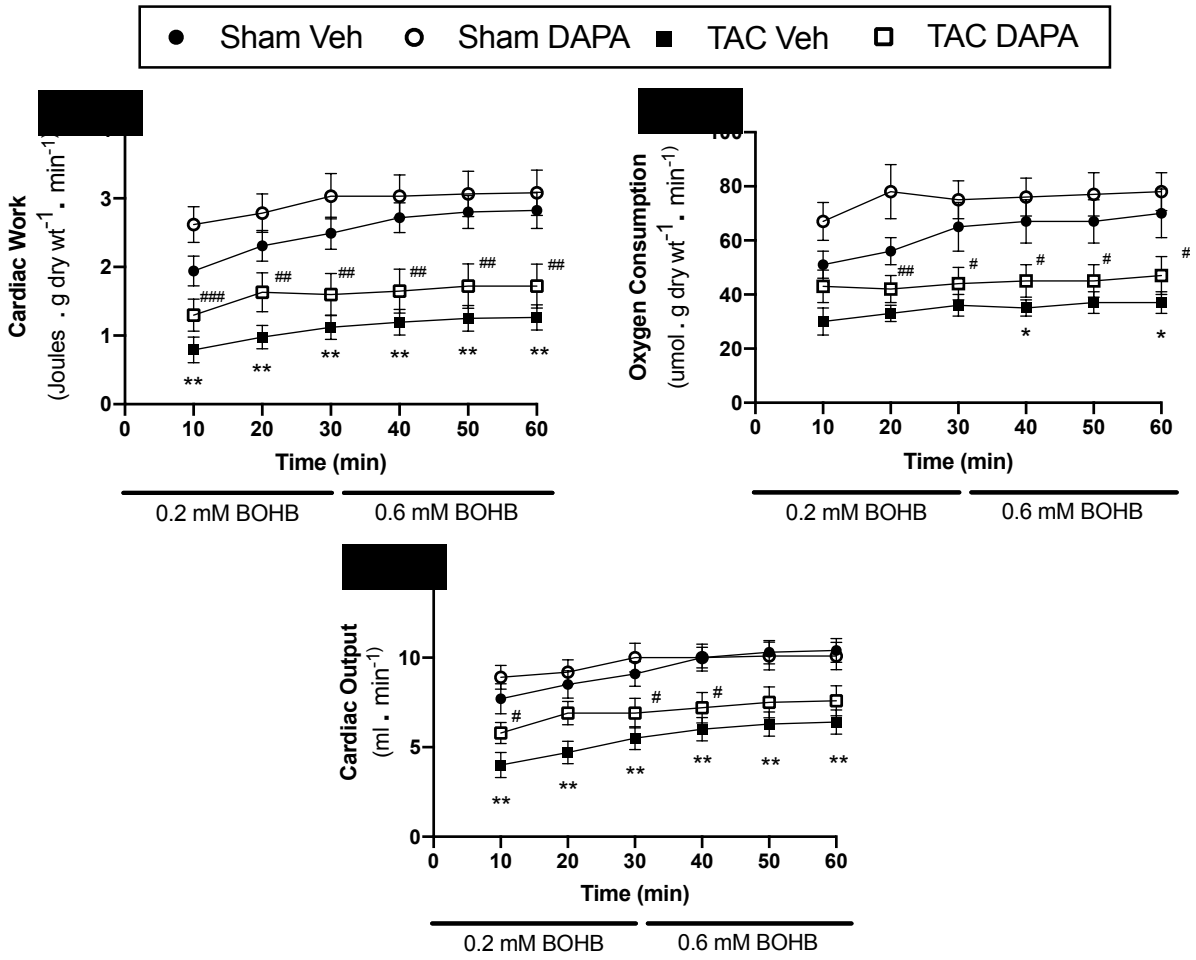

Figure 6. Ex-Vivo Cardiac Function at 0.2 mM BOHB and 0.6 mM BOHB in Sham and TAC Mice Treated with Either Vehicle or Dapagliflozin. *(A)* Cardiac Work (CW) (n = 10-13). *(B)* Oxygen Consumption (n=10-13). *(C)* Cardiac Output (n =10-13). Data are presented as means ± SEM. Data was analyzed by One-Way ANOVA followed by Sidak's multiple-comparison test. $^{*}P < 0.05$ vs Sham Veh, $^{**}P < 0.005$ vs Sham Veh, $^{***}P < 0.0005$ vs Sham Veh, $^{****}P < 0.0001$ vs Sham Veh. $^{\#}P < 0.05$ vs Sham DAPA, $^{\#\#}P < 0.005$ vs Sham DAPA, $^{\#\#\#}P < 0.0005$ vs Sham DAPA, $^{\#\#\#\#}P < 0.0001$ vs Sham DAPA. $^{\dagger}P < 0.05$ vs TAC VEH. DAPA, Dapagliflozin; Veh, Vehicle.

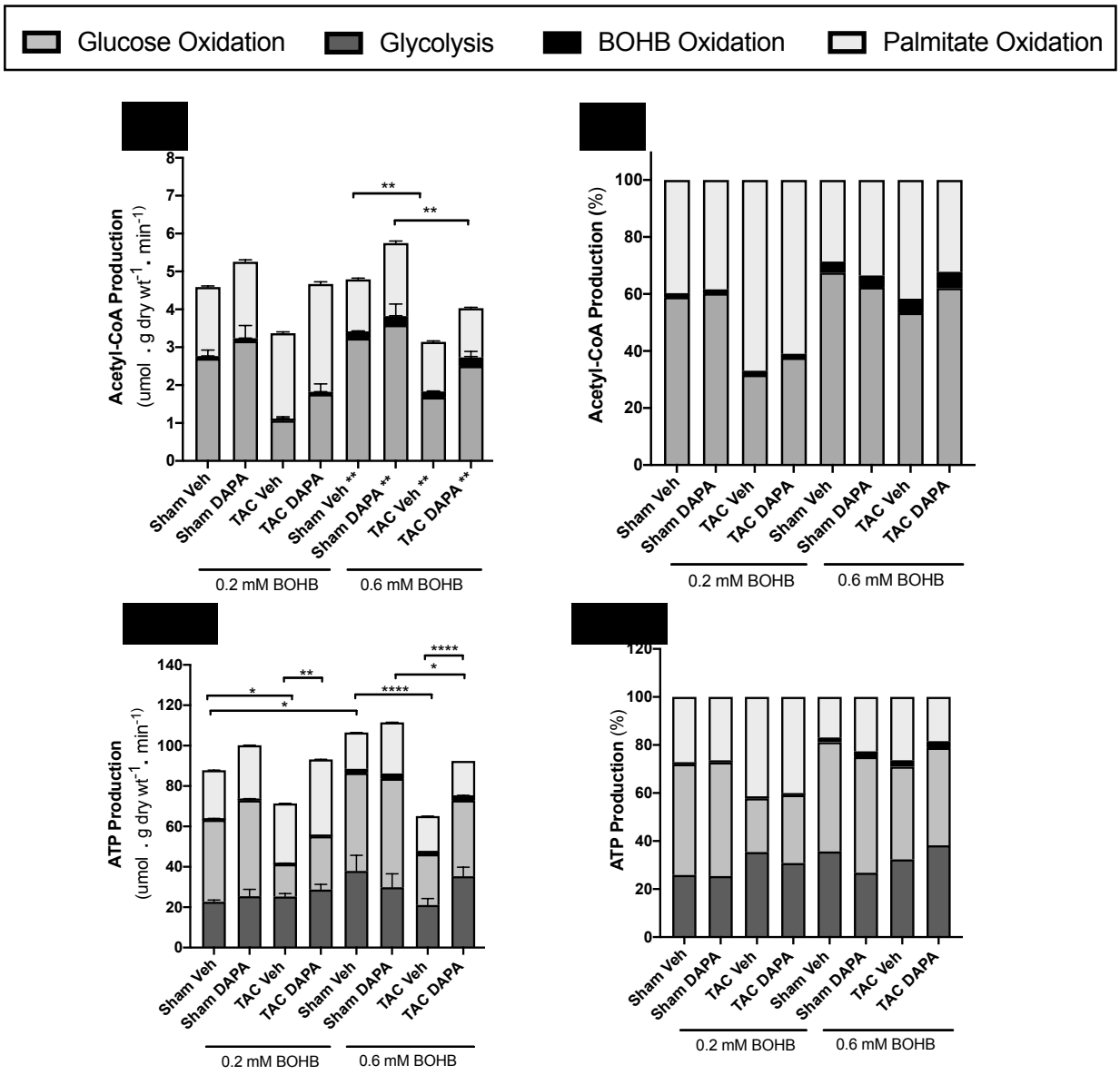

Figure 7. Acetyl-CoA and ATP Production at 0.2 mM BOHB and 0.6 mM BOHB in Sham and TAC Mice Treated with Either Vehicle or Dapagliflozin. *(A)* Acetyl-CoA Production (n = 10-13). *(B) %* Acetyl-CoA Production (n = 10-13). *(C)* ATP Production (n = 10-13). *(D) %* ATP Production (n = 10-13). Data are presented as means ± SD for A and C; means ± SEM for B and D. Data was analyzed by One-Way ANOVA followed by Sidak's multiple-comparison test. $^{*}P < 0.05$, $^{**}P < 0.005$, $^{***}P < 0.0005$, $^{****}P < 0.0001$. DAPA, Dapagliflozin; Veh, Vehicle.

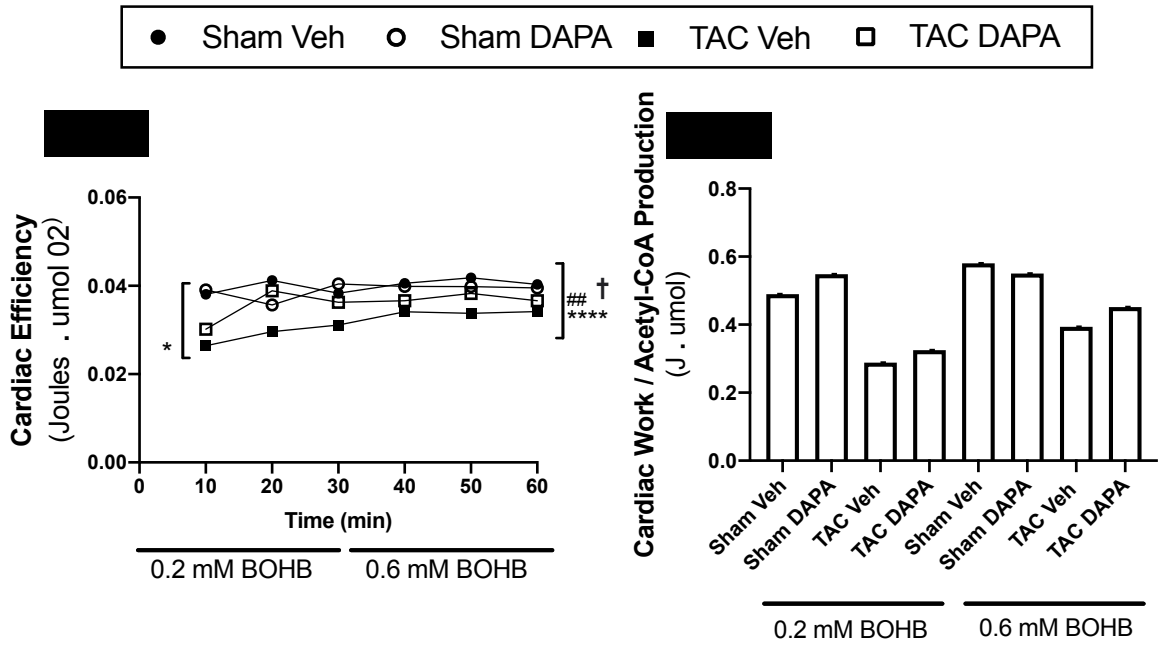

Figure 8. Cardiac Efficiency in Sham and TAC Mice Treated with Either Vehicle or Dapagliflozin. *(A)* Cardiac Efficiency (n = 10-13). *(B)* Cardiac Work Normalized to Acetyl-CoA Production (n = 10-13). Data are presented as means for A and B. Data was analyzed by One-Way ANOVA followed by Sidak's multiple-comparison test. $^{*}P < 0.05$ vs Sham Veh, $^{**}P < 0.005$ vs Sham Veh, $^{***}P < 0.0005$ vs Sham Veh, $^{****}P < 0.0001$ vs Sham Veh. $^{\#}P < 0.05$ vs Sham DAPA, $^{\#\#}P < 0.005$ vs Sham DAPA, $^{\#\#\#}P < 0.0005$ vs Sham DAPA, $^{\#\#\#\#}P < 0.0001$ vs Sham DAPA. $^{\dagger}P < 0.05$ vs TAC VEH. DAPA, Dapagliflozin; Veh, Vehicle.

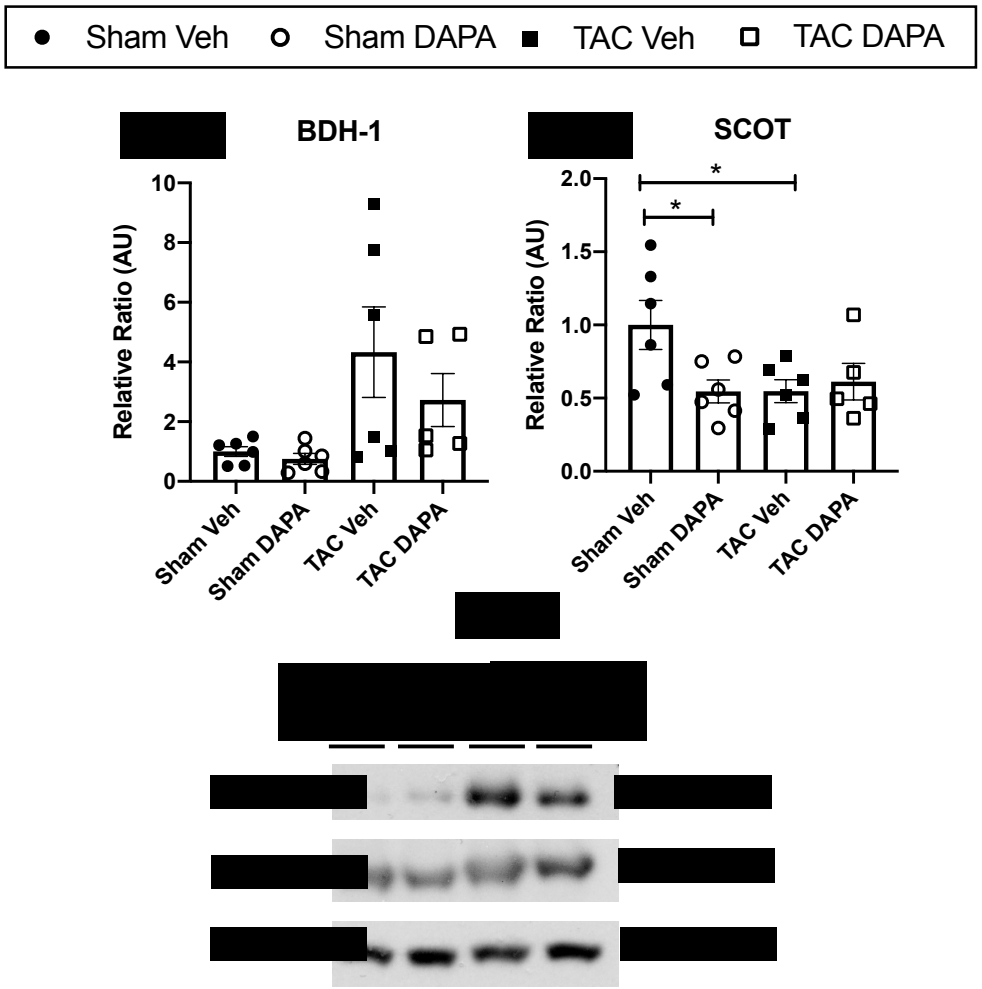

Figure 9. Protein Expression Levels of Ketone Body Oxidative Enzymes in Sham and TAC Mice Treated with Either Vehicle or Dapagliflozin. *(A)* Betahydroxybutyrate dehydrogenase 1 (BDH-1) (n = 5-6). *(B)* Succinyl-CoA-3-oxaloacid CoA transferase (SCOT) (n = 5-6). *(C)* Densitometric analysis (n = 6). Data are presented as means ± SEM. Data was analyzed by One-Way ANOVA followed by Sidak's multiple-comparison test. $^{*}P < 0.05$, DAPA, Dapagliflozin; Veh, Vehicle.

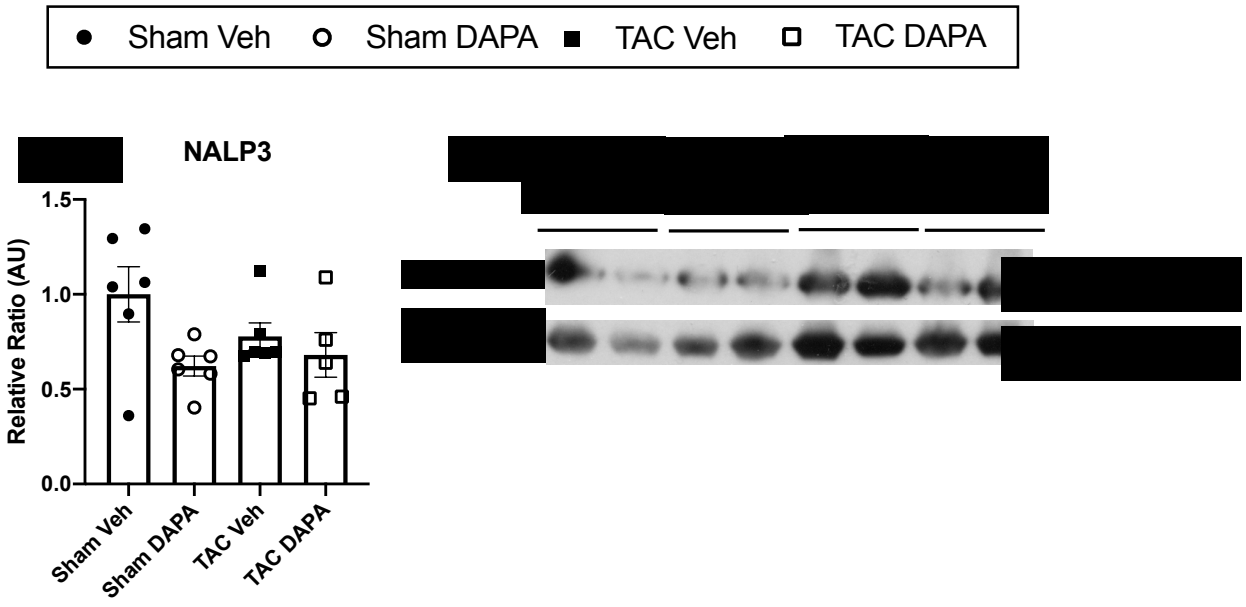

Figure 10. Protein Expression Levels of NRLP3/NALP3 Inflammasome in Sham and TAC Mice Treated with Either Vehicle or Dapagliflozin. *(A)* Nod like receptor protein family 3 (NRLP3/NALP3) (n = 6). *(B)* Densitometric analysis (n = 6). Data are presented as means ± SEM. Data was analyzed by One-Way ANOVA followed by Sidak's multiple-comparison test. $^{*}P < 0.05$, DAPA, Dapagliflozin; Veh, Vehicle.

Table 1. Cardiac Function Parameters at Pre and Post Dapagliflozin Treatment in Sham and TAC Mice. LV, left ventricle; LA, left atrium; IVS, Interventricular septum, LVPW, left ventricle posterior wall; LVID, left ventricle internal diameter; LVEDV, left ventricle end-diastolic volume; LVESV, left ventricle end-systolic volume; HR, heart rate; E, early mitral inflow; A, late mitral inflow; e', tissue Doppler mitral annulus velocity in late diastole; a', tissue Doppler mitralannulus velocity in early diastole; IVRT, isovolumic relaxation time; mg, milligrams; mm, millimeters; µl, microliters; bpm, beats per minute; ms, millisecond; s, second. Data are presented as means ± SD (n=7-13 for each group). Data was analyzed by One-Way ANOVA followed by Sidak's multiple-comparison test. $^{*}P < 0.05$ vs Sham Veh pre-treatment, $^{**}P < 0.005$ vs Sham Veh pre-treatment, $^{***}P < 0.0005$ vs Sham Veh pre-treatment, $^{****}P < 0.0001$ vs Sham Veh pre-treatment. $^{\#}P < 0.05$ vs Sham DAPA pre-treatment, $^{\#\#}P < 0.005$ vs Sham DAPA pre-treatment, $^{\#\#\#}P < 0.0005$ vs Sham DAPA pre-treatment, $^{\#\#\#\#}P < 0.0001$ vs Sham DAPA pre-treatment. $^{\dagger}P < 0.05$ vs Sham Veh post-treatment, $^{\dagger\dagger}P < 0.005$ vs Sham Veh post-treatment, $^{\dagger\dagger\dagger}P < 0.0005$ vs Sham Veh post-treatment, $^{\dagger\dagger\dagger\dagger}P < 0.0001$ vs Sham Veh post-treatment. $^{¥}P < 0.05$ vs Sham DAPA post-treatment, $^{¥¥}P < 0.005$ vs Sham DAPA post-treatment, $^{¥¥¥}P < 0.0005$ vs Sham DAPA post-treatment, $^{¥¥¥¥}P < 0.0001$ vs Sham DAPA post-treatment.

	Pre-treatment				Post-treatment			
	Sham Veh	Sham DAPA	TAC Veh	TAC DAPA	Sham Veh	Sham DAPA	TAC Veh	TAC DAPA
HR (bpm)	439.83±30	415.79±39	451.38±59	446.16±43	409.08±34	407.11±46	451.83±59	445.01±57
Morphology								
LV mass (mg)	64.77±10.2	58.22±15.2	107.91±28.0 *	93.65±25.4	69.22±15.7	62.87±9.6	125.86±49.6 ††	107.59±41.9 ¥¥
LA size (mm)	1.80±0.1	1.68±0.2	2.04±0.4	2.12±0.3	1.87±0.2	1.72±0.2	2.19±0.5	2.06±0.4
IVS diastole (mm)	0.60±0.06	0.54±0.07	0.81±0.14 ***	0.74±0.13 ###	0.60±0.09	0.58±0.05	0.81±0.14 ††	0.75±0.12 ¥¥
LVPW diastole (mm)	0.60±0.07	0.57±0.07	0.83±0.15 **	0.76±0.11 ##	0.58±0.05	0.58±0.06	0.82±0.18 †††	0.76±0.11 ¥¥
LVID diastole (mm)	3.99±0.2	3.96±0.4	4.22±0.3	4.15±0.3	4.17±0.3	4.02±0.3	4.59±0.6	4.42±0.6
LVID systole (mm)	2.85±0.2	2.86±0.5	3.57±0.4 *	3.41±0.4	2.97±0.3	2.91±0.2	4.12±0.7 †††	3.80±0.8 ¥¥¥
Systolic Function								
Ejection Fraction (%)	55.14±2.8	54.95±7.8	33.60±8.9 ****	37.31±8.4 ####	54.46±3.7	54.33±3.7	27.71±10.0 ††††	31.94±9.9 ¥¥¥¥
Fractional Shortening (%)	28.27±1.8	28.34±5.3	15.93±4.7 ****	17.88±4.6 ####	27.94±2.3	27.78±2.4	12.99±4.9 ††††	15.12±5.0 ¥¥¥¥
LVEDV (µl)	70.32±7.7	70.37±12.3	80.62±14.0	75.66±14.5	78.63±12.3	71.71±11.0	101.76±29.2	90.93±32.5
LVESV (µl)	31.67±4.8	32.41±10.0	54.28±15.4	47.77±13.1	36.04±7.4	32.82±6.2	75.96±33.6 ††	64.55±33.3 ¥¥
Diastolic Function								
E (mm/s)	631.34±61	587.67±93	615.29±120	609.29±162	635.45±85	594.42±82	637.74±156	676.27±137
A (mm/s)	357.54±51	349.22±75	407.49±131	337.48±128	326.26±105	319.43±81	304.60±106	362.40±103
e' (mm/s)	-27.01±4.8	-24.20±4.8	-17.98±8.4	-23.23±10.6	-27.37±2.6	-22.90±4.8	-21.18±8.1	-17.29±6.7
a' (mm/s)	-21.22±2.6	-18.18±3.8	-14.29±6.8	-16.47±8.9	-18.82±2.8	-17.39±3.6	-13.29±5.9	-13.75±7.3
E/A ratio	1.81±0.38	1.72±0.29	1.58±0.36	1.92±0.60	2.11±0.62	1.94±0.43	2.22±0.68	1.98±0.58
E/e' ratio	23.74±3.1	24.96±5.5	40.96±17.4	32.70±15.1	23.46±4.1	26.68±4.7	32.30±10.1	43.92±15.2
E/E'	-23.74±3.06	-24.95±5.45	-41.39±16.95 *	-36.168±16.5	-23.46±4.11	-26.67±4.7	-34.75±9.83	-48.47±17.8 ¥¥¥¥
IVRT (ms)	11.73±3.5	12.69±2.6	15.12±2.6	15.24±3.6	12.24±2.9	12.24±2.9	14.43±2.3	14.20±4.0

Table 2. Ex-Vivo Cardiac Function Parameters at 0.2 mM BOHB and 0.6 mM BOHB in Sham and TAC Mice Treated with Either Vehicle or Dapagliflozin. Data are presented as means ± SEM (n= 3-6 for each group). Data was analyzed by One-Way ANOVA followed by Sidak's multiple-comparison test. $^{*}P < 0.05$ vs Sham Veh pre-treatment, $^{**}P < 0.005$ vs Sham Veh pre-treatment, $^{***}P < 0.0005$ vs Sham Veh pre-treatment, $^{****}P < 0.0001$ vs Sham Veh pre-treatment. $^{\#}P < 0.05$ vs Sham DAPA pre-treatment, $^{\#\#}P < 0.005$ vs Sham DAPA pre-treatment, $^{\#\#\#}P < 0.0005$ vs Sham DAPA pre-treatment, $^{\#\#\#\#}P < 0.0001$ vs Sham DAPA pre-treatment. $^{\dagger}P < 0.05$ vs Sham Veh post-treatment, $^{\dagger\dagger}P < 0.005$ vs Sham Veh post-treatment, $^{\dagger\dagger\dagger}P < 0.0005$ vs Sham Veh post-treatment, $^{\dagger\dagger\dagger\dagger}P < 0.0001$ vs Sham Veh post-treatment. $^{¥}P < 0.05$ vs Sham Veh post-treatment, $^{¥¥}P < 0.005$ vs Sham Veh post-treatment, $^{¥¥¥}P < 0.0005$ vs Sham Veh post-treatment, $^{¥¥¥¥}P < 0.0001$ vs Sham Veh post-treatment. $^{¢}P < 0.05$ vs TAC Veh post-treatment, $^{¢¢}P < 0.005$ vs TAC Veh post-treatment, $^{¢¢¢}P < 0.0005$ vs TAC Veh post-treatment, $^{¢¢¢¢}P < 0.0001$ vs TAC Veh post-treatment.

			0.2 mM βOHB				0.6 mM βOHB	
	Sham Veh	Sham DAPA	TAC Veh	TAC DAPA	Sham Veh	Sham DAPA	TAC Veh	TAC DAPA
HR (HR; bpm)	291±11	279±12	225±12 **	229±15	276±9	282±15	221±9 *	245±13
Peak systolic pressure (PSP)	70±0.8	72±1.0	71±1.6	71±1.1	71±0.9	72±1.1	71±1.1	71±1.0
Developed pressure (DP)	22±1.1	25±1.5	21±2.3	22±1.3	23±1.0	25±1.5	23±1.4	25±1.1
HR x PSP ($x\ 10^{-3}$)	20±0.0	20±0.9	16±1.0 *	16±1.0 #	20±0.8	20±1.1	16±0.7 †	17±0.9
HR x DP ($x\ 10^{-3}$)	6±0.3	7±0.5	5±0.5	5±0.3	6±0.3	7±0.6	5±0.4	6±0.4
Cardiac output ($ml \cdot min^{-1}$)	8.4±0.74	9.4±0.69	4.8±0.6 **	6.1±0.6 #	10.2±0.62	10.1±0.77	6.2±0.67 **	7.3±0.68
Aortic output ($ml \cdot min^{-1}$)	6.4±0.68	7.1±0.65	3.3±0.55 *	4.7±0.71	7.8±0.48	7.8±0.79	4.6±0.57 †	5.9±0.79
Coronary flow ($ml \cdot min^{-1}$)	2.1±0.16	2.3±0.08	1.4±0.11 *	2.1±0.19	2.4±0.22	2.3±0.1	1.6±0.17 ††	2.1±0.18
Cardiac work ($J \cdot min^{-1} \cdot g\ dry\ wt^{-1}$)	2.25±0.21	2.81±0.28	0.97±0.17 **	1.56±0.27 ##	2.78±0.24	3.068±0.32	1.24±0.19 ††	1.85±0.31 ¥¥
Oxygen consumption per g dry wt ($\mu mol \cdot min^{-1} \cdot g\ dry\ wt^{-1}$)	57±6	73±7	33±3	43±5 #	68±8	77±7	36±4 †	46±6 ¥
Cardiac efficiency (Joules · µmol 02)	0.0392	0.0389	0.0291 *	0.0351	0.0409	0.0397	0.0340 ††††	0.0371 ¥¥ ¢

Chapter Four

DISCUSSION AND CONCLUSIONS

4.1 General Discussion

While SGLT2i have been approved as a treatment approach for T2D, recent large-scale clinical trials have shown SGLT2i confer advantageous cardioprotective effects in both T2D and non-diabetic patients with HF [135-139]. The EMPAREG-OUTCOME trial was the first to show these beneficial cardioprotective effects on T2D patients with established cardiovascular disease [135], with the CANVAS [136] and DECLARE-TIMI [137] trials following shortly after with supporting results, and most recently the DAPA-HF [138] and EMPEROR-REDUCED [139] trials showing this cardioprotection regardless of the presence of T2D alongside HF. In this study, we aimed to determine whether the beneficial cardioprotective effects conferred by SGLT2i in non-diabetic HF are due to providing the energy starved failing heart an extra source of fuel in the form of ketones. We used a murine model of pressure overload hypertrophy HF, induced through transverse aortic constriction surgery, to achieve our objectives. We hypothesized that dapagliflozin will improve cardiac function in a pressure overload hypertrophy HF rodent model, and that the beneficial effects of SGLT2i in the failing heart are mediated through increasing energy supply in the form of ketones. We established pressure overload hypertrophy over 3 weeks in 8-week old C57BL6/N mice, confirmed through the significant drop in systolic parameters: %EF and %FS in TAC hearts **(Figure 3A, 3B, Table 1)**, and the significant increase in markers of hypertrophy: LVPW:d and IVS:d in TAC hearts **(Table 1).** Sham and TAC mice were treated with either dapagliflozin in their drinking water, or vehicle (i.e. regular drinking water without treatment) daily for 4 weeks, following which hearts were subjected to echocardiography and ex vivo isolated working heart perfusions to assess cardiac function and substrate metabolic rates.

Firstly, our results confirmed impairments in cardiac function, fuel use, and bioenergetics in a TAC model of HF. TAC induces hypertrophy and HFrEF [154, 155], and our study confirmed impairments in systolic function through echocardiography assessment **(Figure 3).** Here, we showed lower cardiac function 6 weeks following TAC surgery, through lowered systolic and diastolic function and increased hypertrophy **(Figure 3 and Table 1).** This is in accordance with

previous studies, including our own [148, 156, 157]**.** It has been established that cardiac mitochondrial oxidative phosphorylation decreases in heart failure and the heart reverts towards a more fetal like state, where glycolysis becomes a significant source of energy with significantly decreased glucose oxidation [29, 31, 32, 34, 35, 76, 98]**.** We observed a decrease in absolute glucose oxidation rates in TAC hearts compared to sham hearts **(Figure 4A),** further confirming the impairment of glucose oxidation that occurs in the failing heart**.** Furthermore, we also saw an increase in absolute palmitate oxidation rates with TAC compared to sham **(Figure 4D)**, and when normalized per unit work, palmitate oxidation rates were significantly higher in TAC hearts compared to sham **(Figure 5D).** Glycolytic rates normalized to cardiac work were also higher in TAC hearts **(Figure 5B).** Circulating ketone body levels and cardiac ketone body utilization is known to increase in the failing heart [117-120, 123]**.** Our results confirmed this, as we observed a significant increase in ketone oxidation rates per unit work in TAC hearts compared to sham **(Figure 5C),** as well as an increased protein expression of BDH-1 **(Figure 9A)**. Due to an impairment in cardiac mitochondrial oxidative phosphorylation through the significant drop in glucose oxidation, the heart has to rely on an energy inefficient fuel source, fatty acids [29, 32, 34, 35, 75, 76, 98, 113]**.** This leads to a drop in cardiac efficiency. We observed an impairment in cardiac efficiency **(Figure 8A)** as well as impaired ex vivo cardiac function parameters of cardiac work, oxygen consumption, cardiac output in TAC hearts **(Figure 6 and Table 2).** The failing heart is energy starved as it is not able to produce such a high amount of energy required to sustain contractile function [69, 72, 81, 82]**.** Our results confirmed a significant decrease in total acetyl-CoA and total ATP production in the failing heart **(Figure 7A and C).** Combined, this supports the cardiac energy profile in HF described in previous literature including what we have reported before in our own studies [80], providing further evidence of impaired glucose oxidation in HF.

Interestingly, and much to our surprise, we did not observe certain results which we expected to observe from SGLT2 inhibition. SGLT2i act through increasing glucose excretion, leading to lower blood glucose levels, blood pressure, and body weight [128, 129]. We did not observe a drop in body weight in TAC DAPA mice over 3 weeks of dapagliflozin treatment **(Figure 1A and B)**, nor did we observe a significant reduction in fed and fasting glucose levels in Sham DAPA and TAC DAPA hearts **(Figure 2D-F).** Additionally, we did not observe an improvement

in cardiac function, assessed by echocardiography, in both Sham and TAC mice treated with dapagliflozin **(Figure 3 and Table 1).** We observed some protection of dapagliflozin ex vivo where cardiac efficiency was significantly improved in TAC hearts **(Figure 8A)**; however, this did not translate into an improvement in in vivo cardiac function. SGLT2i are known to increase circulating ketone body levels secondary to increasing lipolysis and breakdown of fatty acids [133, 149-151]**.** We did not observe a significant increase in fed and fasting circulating ketone levels with dapagliflozin treatment in Sham and TAC mice that we expected to see; however, we did observe a trend towards increased circulating ketones following a 16-hour fast **(Figure 2 A-C).** We did not see any benefits and significant improvement in in vivo cardiac function in HF, although we confirmed the presence of HF. We speculate that these results can be due to a variety of reasons. A possible explanation is that the dose of dapagliflozin used (1 mg/kg/bw daily) was not high enough to observe a significant benefit in SGLT2 inhibition. Studies have used 1.5 mg/kg/bw/day and 10 mg/kg/bw/day doses of dapagliflozin [158-161]. However, numerous other studies used the same dose of 1 mg/kg/bw that we used in our study and observed cardioprotection through attenuation of LV posterior wall thickness, %EF, and %FS [140, 157, 162-164]. Additionally, Byrne et al. also failed to observe an increase in circulating ketone levels with SGLT2 inhibition and HF [148]. Another less likely but potential explanation is the dapagliflozin we received from Cayman Chemical may not have been a functional batch and there could have been something wrong with it. While our results do not correlate with previous literature, another possible explanation is that our model of pressure overload hypertrophy induced through TAC may not be a completely accurate representation of the patient population with HFrEF. TAC may not completely recapitulate what happens in vivo with HF in humans. HF is a complex syndrome of multiple aetiologies, and can manifest in a myriad of ways, one of which is hypertrophy and pressure overload [165]**.** Constriction of the transverse aorta results in pressure-overload, which causes the left ventricle to require greater contractile force to pump blood, and as a result the heart developing left ventricular hypertrophy [166]. With prolonged pressure-overload, the heart can decompensate and progress to dilated cardiomyopathy, characterized by impaired systolic function and hypertrophic remodelling. HFrEF can also be characterized by neurohormonal activation, adverse myocardial remodelling, inflammation, and cardiomyopathy to name a few [167-169]. By not showing any improvement in in vivo cardiac function with dapagliflozin, hence no cardioprotective effect, our data does not

fit with clinical data in HFrEF [135, 137-139]**.** Other studies using empagliflozin or dapagliflozin saw cardioprotection in both a diabetic and non-diabetic model of HF [158, 160, 161]; therefore, we are unsure why our results contradict what has been seen in previous literature, other than the possibility of the TAC model of pressure overload hypertrophy HF not fully recapitulating HFrEF in human patients with HF.

However, given these unfortunate results, we did, in fact, see some proof of dapagliflozin treatment working in our model of HF. We observed a significant drop in body weight over 3 weeks of dapagliflozin treatment in the Sham DAPA mice compared to Sham vehicle mice (**Figure 1A).** Although not significant, we did observe a trend towards high blood ketone levels in a fasted state with DAPA **(Figure 2C).** Most importantly, chronic 3-week dapagliflozin treatment significantly improved cardiac efficiency in TAC mice when hearts were perfused with a ketone concentration seen in vivo with dapagliflozin treatment **(Figure 8A),** alongside significantly improving total ATP production in both Sham and TAC mice compared to their vehicle controls **(Figure 7A).** These results suggest that dapagliflozin was present and could be acting according to its function in our model.

Our study also showed very interesting results when it came to the assessment of substrate oxidation rates and total ATP production. Although they were not significant, absolute glucose oxidation rates showed an increased trend with dapagliflozin treatment in TAC hearts when perfused at both 0.2 mM and 0.6 mM BOHB, and absolute BOHB oxidation rates showed an increased trend with dapagliflozin treatment when perfused at 0.6 mM BOHB **(Figure 4A and C).** This increase in glucose and BOHB oxidation may account for the significant increase in overall ATP production and non significant increase in acetyl-CoA production observed with dapagliflozin treatment in TAC hearts at both BOHB concentrations **(Figure 7C).** Furthermore, we observed that dapagliflozin treatment in TAC mice resulted in a decreased contribution of palmitate oxidation to total ATP production when hearts were perfused at 0.6 mM BOHB (**Figure 7D).** This, alongside the increase in glucose oxidation rates may account for the significant increase in cardiac efficiency observed in the TAC DAPA hearts when perfused with 0.6 mM ketones.

Next, immunoblotting suggested that BDH-1 protein expression was lower in TAC hearts treated with DAPA **(Figure 9A)**, although BOHB oxidation rates trended higher in TAC hearts treated with DAPA at 0.6 mM BOHB **(Figure 4C and 5C)**. Furthermore, SCOT protein expression was unchanged in TAC DAPA hearts compared to TAC Veh hearts, but lower in Sham DAPA hearts compared to Sham Veh hearts **(Figure 9B).** This is another source of evidence suggesting dapagliflozin treatment worked, and it suggests a possible downregulation of ketone body enzymes with DAPA treatment. Since SGLT2i have also been proposed to exert their cardioprotective effects through modulating inflammation through the NLRP3/NALP3 inflammasome, we assessed the protein expression of the NLRP3/NALP3 inflammasome and saw a trend towards lower NALP3 expression in both DAPA groups **(Figure 10A).** This was more apparent in the Sham DAPA group compared to Sham Veh. This provides further evidence of dapagliflozin function in our study.

Lastly, we observed many interesting and noteworthy results when both the normal and failing heart is exposed to a higher concentration of ketones in the perfusate (i.e. given an extra source of fuel). When provided with an increased fuel supply through ketones, the normal heart oxidizes a significantly greater amount of BOHB **(Figure 4C and 5C).** When provided with an increased fuel supply through ketones, the failing heart also oxidizes a significantly greater amount of BOHB **(Figure 4C and 5C).** This was supported by an increase in BDH-1 protein expression seen in TAC Veh hearts **(Figure 9A).** However, this increase in BOHB oxidation is not at the expense of glucose oxidation, as glucose oxidation rates also slightly increase (non- significant) **(Figure 4A and 5A).** Additionally, palmitate oxidation also decreases with the extra source of ketones **(Figure 4D and 5D).** This was consistent with an increased contribution of ATP from glucose and BOHB oxidation and decreased contribution from palmitate oxidation when hearts were perfused with higher BOHB **(Figure 7D).** These finds show that the heart is able to accommodate for an increased ketone body supply and translate it into increased energy production from this substrate. Together, these suggest that perhaps, when given the choice, the failing heart prefers to utilize the more energy efficient fuel source: ketones. This supports the notion that increasing delivery of ketone bodies to the failing heart could be beneficial and adaptive in the treatment of HF. However, this does not translate into an improvement in cardiac efficiency, as the failing heart is still significantly inefficient compared to the normal heart,

shown through both our results and our previous studies [80-82] **(Figure 8A)**. It is interesting to note that total ATP production did not, however, significantly increase in the failing heart when exposed to a higher concentration of BOHB in the perfusate **(Figure 7C).**

There has been a lack of consensus on the mechanisms through which SGLT2i have their cardioprotective effects in HF. In our present study, we hypothesized that dapagliflozin improves cardiac function by providing the failing heart with an extra source of fuel in the form of ketones. Although we did not observe improvement in in vivo cardiac function, we observed an increase in cardiac efficiency with dapagliflozin treatment in HF, alongside increased ATP production due to increased glucose and BOHB oxidation rates. Although we did see trends similar to our previously published studies [127]**,** we did not observe any significant improvement in cardiac energy metabolism with DAPA at both 0.2 mM and 0.6 mM BOHB. We don't know with full certainty that the dapagliflozin dose was adequate enough to be working; however, if we were to believe that it was working properly in this case, we still did not see a significant increase in plasma ketones in vivo, nor did we see any significant effects on overall cardiac energy metabolism with dapagliflozin treatment. Therefore, our results suggest that the beneficial cardiovascular effects of SGLT2i may not be due to fuel use and improved energetics as hypothesized, as we did not observe any significant changes in substrate oxidative rates with dapagliflozin. It is very important to note that there could also be the possibility of dapagliflozin not working properly in our TAC model of pressure overload hypertrophy HF, but since DAPA showed benefits in the Sham group compared to Sham Veh, it is more likely that dapagliflozin worked, but the cardioprotective mechanism of SGLT2i may not be through our proposed pathway. It is also likely that the murine TAC model of pressure overload hypertrophy HF does not fully recapitulate the full extent of HFrEF observed in human HF. We believe there is value in exploring the NLRP3/NALP3 inflammasome pathway as a potential mechanism through which SGLT2i may be acting. Ketones may inhibit the NLRP3/NALP3 inflammasome directly to exert the beneficial effects of SGLT2i [68, 145, 148]**.** Increasing serum BOHB levels successfully supressed activation of the NLRP3 inflammasome independent of mitochondrial oxidation [68, 148]. We observed a non-significant decrease in NALP3 protein expression in Sham and TAC hearts treated with dapagliflozin, suggesting merit and value in further looking

into the downstream targets of the inflammatory pathway such as interleukin 18 and 1B (IL-18 and IL-1B). Further work is required to assess this.

4.2 Limitations

There are some limitations to the project presented here to discuss. Firstly, we did not measure urinary glucose levels, only blood glucose levels. Measuring urinary glucose levels could have helped elucidate the efficacy of dapagliflozin treatment, as this would have been expected to rise with SGLT2 inhibition. We also did not measure food intake or energy expenditure; this could give us some insight into the behavior of mice from each group, since the TAC mice were probably burning less energy per day. Additionally, we did not measure triglyceride/ free fatty acid or ketone levels in the plasma that we isolated from the blood from the mice at the time of the perfusion. It would be very beneficial to assess these parameters in the plasma to act as another confirmation as to whether Dapa was present and working or not in our model. We would expect both plasma triglycerides/ free fatty acids and ketones to be significantly higher in the mice treated with dapagliflozin compared to the vehicle mice. Additionally, HPLC assays for dapagliflozin could also be done to act as another confirmation. Another limitation is that we administered dapagliflozin through drinking water. With this method of administration, it is difficult to be sure that all the mice received the exact same dose of dapagliflozin. The dosage was calculated and adjusted according to the body weight of the mice and the amount of water the mice were consuming, and the amount of water consumed by the mice per day was also recorded by measuring water levels daily. However, with multiple mice in a given cage, it is possible that the mice received inconsistent dosing or drank more/less water than expected. However, other methods such as oral gavage may provide better results, as the treatment is provided directly into the esophagus. It should be noted that this method can be stressful to both the animal and the individual doing the gavage [170]. Aside from oral gavage, the mice could also have been singly housed; however, this may increase stress in the mice and subsequently affect experiments. Another limitation is that in Figure 9, the representative blot for SCOT did not match its respective graph. Either a different representative blot could be shown for this target, or the loading control could have been changed to assess whether this difference still remains. This would act as a confirmation of whether the trend we observed in SCOT it accurate or not. Finally, the COVID-19 pandemic presented some limitations of its own, resulting in lab

shutdowns during parts of Spring/Summer 2020 and Winter 2020/21. Due to this, some active cohorts had to be postponed and others cancelled, leading to low and passable n numbers in certain cases (such as n of 3 for glycolytic rates). This also resulted in delays in conducting immunoblotting on every target we had aimed. However, given the circumstances, we did the best we could and were able to still achieve a large amount of experiments and data analysis.

4.3 Future Directions

Future directions assessing plasma triglyceride/free fatty acid and plasma ketone levels to confirm the presence and action of dapagliflozin. Another future direction includes further exploring the effect of dapagliflozin on the NLRP3/NALP3 inflammasome pathway in a pressure overload hypertrophy model of HF as a potential mediator of cardiac improvements with SGLT2i. We observed a trend towards lowered NALP3 protein expression with dapagliflozin treatment; therefore, it would be very interesting and revealing to see what the effect on downstream targets such as IL-18 and IL-1B would be, alongside the other components of the inflammasome: ASC and caspase-1. Fibrotic and apoptotic markers would also be something important and interesting to look at. This study can also be done in different models of HF that are closer in recapitulating HFrEF as in humans, or also in other forms of HF aside from HFrEF. HFpEF is another common form of HF. It would be very worthwhile to assess whether SGLT2i have any cardioprotection in this condition and determine a possible mechanism, alongside determining whether ketones can still provide an extra source of fuel and increase total ATP production in theis form of HF. Lastly, even though we did not observe any cardioprotection in our study, the effect of SGLT2i in priming the heart prior to HF could be a potential avenue in determining whether SGLT2i could have beneficial effects in individuals at high risk for cardiovascular disease, but do not currently have major cardiovascular disease or HF, and possibly are pre-diabetic.

4.4 Conclusions

In conclusion, our study results did not show a cardioprotective effect from dapagliflozin as dapagliflozin did not improve in vivo cardiac function in a TAC model of pressure-overload hypertrophy HF. However, we did observe an improvement in ex vivo function through an increase in cardiac efficiency alongside increased total ATP production, which can be attributed

to an increase in glucose and BOHB oxidation rates. We did not observe any significant improvements in substrate metabolic rates. Therefore, is is possible that dapagliflozin's cardioprotective benefits may be independent of metabolism.

BIBLIOGRAPHY

1. Organization, W.H., *Noncommunicable diseases country profiles 2018.* 2018.
2. Cowie, M., et al., *The epidemiology of heart failure.* European heart journal, 1997. **18**(2): p. 208-225.
3. McMurray, J.J. and S. Stewart, *The burden of heart failure.* European Heart Journal Supplements, 2002. **4**(suppl_D): p. D50-D58.
4. Roger, V.L., et al., *Trends in heart failure incidence and survival in a community-based population.* Jama, 2004. **292**(3): p. 344-350.
5. Wang, G., et al., *Costs of heart failure-related hospitalizations in patients aged 18 to 64 years.* The American journal of managed care, 2010. **16**(10): p. 769-776.
6. Physicians, D.i.C.W.t.A.C.o.C., et al., *ACC/AHA 2005 guideline update for the diagnosis and management of chronic heart failure in the adult—summary article: a report of the American College of Cardiology/American Heart Association Task Force on Practice Guidelines (Writing Committee to Update the 2001 Guidelines for the Evaluation and Management of Heart Failure).* Journal of the American College of Cardiology, 2005. **46**(6): p. 1116-1143.
7. Hunt, S., *Baker DW, Chin MH, Cinquegrani MP, Feldman AM, Francis GS, Ganiats TG, Goldstein S, Gregoratos G, Jessup MK, Noble RJ, Packer M, Silver MA, Stevenson LW.* ACC/AHA guidelines for the evaluation and management of chronic heart failure in the adult: executive summary. Circulation, 2001. **104**: p. 2996-3007.
8. Simmonds, S.J., et al., *Cellular and molecular differences between HFpEF and HFrEF: a step ahead in an improved pathological understanding.* Cells, 2020. **9**(1): p. 242.
9. Angeja, B.G. and W. Grossman, *Evaluation and management of diastolic heart failure.* Circulation, 2003. **107**(5): p. 659-663.
10. Aurigemma, G.P. and W.H. Gaasch, *Diastolic heart failure.* New England Journal of Medicine, 2004. **351**(11): p. 1097-1105.
11. Little, W.C. and R.J. Applegate, *Congestive heart failure: systolic and diastolic function.* Journal of cardiothoracic and vascular anesthesia, 1993. **7**(4): p. 2-5.
12. Davie, A., et al., *Value of the electrocardiogram in identifying heart failure due to left ventricular systolic dysfunction.* BMJ: British Medical Journal, 1996. **312**(7025): p. 222.

13. Redfield, M.M., et al., *Burden of systolic and diastolic ventricular dysfunction in the community: appreciating the scope of the heart failure epidemic.* Jama, 2003. **289**(2): p. 194-202.
14. Konstam, M.A., *Heart failure: evaluation and care of patients with left-ventricular systolic dysfunction*. 1994: US Department of Health and Human Services, Public Health Service, Agency ….
15. Yancy, C.W., et al., *2013 ACCF/AHA guideline for the management of heart failure: executive summary: a report of the American College of Cardiology Foundation/American Heart Association Task Force on practice guidelines.* Circulation, 2013. **128**(16): p. 1810-1852.
16. Kannel, W.B. and D.L. McGee, *Diabetes and cardiovascular disease: the Framingham study.* Jama, 1979. **241**(19): p. 2035-2038.
17. Ho, K.K., et al., *The epidemiology of heart failure: the Framingham Study.* Journal of the American College of Cardiology, 1993. **22**(4S1): p. A6-A13.
18. Association, A.D., *Screening for diabetes.* Diabetes care, 2002. **25**(suppl 1): p. s21-s24.
19. Association, A.D., *9. Pharmacologic approaches to glycemic treatment: Standards of Medical Care in Diabetes—2020.* Diabetes care, 2020. **43**(Supplement 1): p. S98-S110.
20. Haffner, S.M., et al., *Mortality from coronary heart disease in subjects with type 2 diabetes and in nondiabetic subjects with and without prior myocardial infarction.* New England journal of medicine, 1998. **339**(4): p. 229-234.
21. Smith, J.W., et al., *Prognosis of patients with diabetes mellitus after acute myocardial infarction.* The American journal of cardiology, 1984. **54**(7): p. 718-721.
22. Das, S.R., et al., *Effects of diabetes mellitus and ischemic heart disease on the progression from asymptomatic left ventricular dysfunction to symptomatic heart failure: a retrospective analysis from the Studies of Left Ventricular Dysfunction (SOLVD) Prevention trial.* American heart journal, 2004. **148**(5): p. 883-888.
23. De Groote, P., et al., *Impact of diabetes mellitus on long-term survival in patients with congestive heart failure.* European heart journal, 2004. **25**(8): p. 656-662.
24. Ingwall, J.S., *ATP and the Heart*. Vol. 11. 2002: Springer Science & Business Media.
25. Opie, L., *Cardiac metabolism–emergence, decline, and resurgence. Part I.* Cardiovascular research, 1992. **26**(8): p. 721-733.

26. Stanley, W.C., F.A. Recchia, and G.D. Lopaschuk, *Myocardial substrate metabolism in the normal and failing heart.* Physiological reviews, 2005. **85**(3): p. 1093-1129.
27. Bing, R., et al., *Metabolism of the human heart: II. Studies on fat, ketone and amino acid metabolism.* The American journal of medicine, 1954. **16**(4): p. 504-515.
28. Wisneski, J.A., et al., *Myocardial metabolism of free fatty acids. Studies with 14C-labeled substrates in humans.* The Journal of clinical investigation, 1987. **79**(2): p. 359-366.
29. Lopaschuk, G.D., et al., *Regulation of fatty acid oxidation in the mammalian heart in health and disease.* Biochimica et Biophysica Acta (BBA)-Lipids and Lipid Metabolism, 1994. **1213**(3): p. 263-276.
30. van der Vusse, G.J., M. van Bilsen, and J.F. Glatz, *Cardiac fatty acid uptake and transport in health and disease.* Cardiovascular research, 2000. **45**(2): p. 279-293.
31. Karwi, Q.G., et al., *Loss of metabolic flexibility in the failing heart.* Frontiers in cardiovascular medicine, 2018. **5**: p. 68.
32. Stanley, W.C., et al., *Regulation of myocardial carbohydrate metabolism under normal and ischaemic conditions: potential for pharmacological interventions.* Cardiovascular research, 1997. **33**(2): p. 243-257.
33. Taegtmeyer, H., *Energy metabolism of the heart: from basic concepts to clinical applications applications.* Current problems in cardiology, 1994. **19**(2): p. 61-113.
34. Lopaschuk, G.D., *Metabolic modulators in heart disease: past, present, and future.* Canadian Journal of Cardiology, 2017. **33**(7): p. 838-849.
35. Lopaschuk, G.D., et al., *Myocardial fatty acid metabolism in health and disease.* Physiological reviews, 2010. **90**(1): p. 207-258.
36. Taegtmeyer, H., *Cardiac metabolism as a target for the treatment of heart failure*. 2004, Am Heart Assoc.
37. Taegtmeyer, H., *Principles of fuel metabolism in heart muscle.* Myocardial energy metabolism, 1988: p. 17-34.
38. Randle, P., et al., *The glucose fatty-acid cycle its role in insulin sensitivity and the metabolic disturbances of diabetes mellitus.* The lancet, 1963. **281**(7285): p. 785-789.
39. TURNER, J.F. and D.H. TURNER, *The regulation of glycolysis and the pentose phosphate pathway*, in *Metabolism and Respiration*. 1980, Elsevier. p. 279-316.

40. WU, P., et al., *Starvation and diabetes increase the amount of pyruvate dehydrogenase kinase isoenzyme 4 in rat heart.* Biochemical Journal, 1998. **329**(1): p. 197-201.
41. Waters, E., J.P. Fletcher, and I.A. Mirsky, *The relation between carbohydrate and ß-hydroxybutyric acid utilization by the heart-lung preparation.* American Journal of Physiology-Legacy Content, 1938. **122**(2): p. 542-546.
42. Mitchell, G., et al., *Medical aspects of ketone body metabolism.* Clinical and investigative medicine. Medecine clinique et experimentale, 1995. **18**(3): p. 193-216.
43. Balasse, E.O. and F. Féry, *Ketone body production and disposal: effects of fasting, diabetes, and exercise.* Diabetes/metabolism reviews, 1989. **5**(3): p. 247-270.
44. Fukao, T., G.D. Lopaschuk, and G.A. Mitchell, *Pathways and control of ketone body metabolism: on the fringe of lipid biochemistry.* Prostaglandins, leukotrienes and essential fatty acids, 2004. **70**(3): p. 243-251.
45. Cotter, D.G., R.C. Schugar, and P.A. Crawford, *Ketone body metabolism and cardiovascular disease.* American Journal of Physiology-Heart and Circulatory Physiology, 2013.
46. Halestrap, A.P. and N.T. PRICE, *The proton-linked monocarboxylate transporter (MCT) family: structure, function and regulation.* Biochemical Journal, 1999. **343**(2): p. 281-299.
47. Owen, O., et al., *Brain metabolism during fasting.* The Journal of clinical investigation, 1967. **46**(10): p. 1589-1595.
48. Halestrap, A.P., *The monocarboxylate transporter family—structure and functional characterization.* IUBMB life, 2012. **64**(1): p. 1-9.
49. Halestrap, A.P. and M.C. Wilson, *The monocarboxylate transporter family—role and regulation.* IUBMB life, 2012. **64**(2): p. 109-119.
50. Owen, O.E., et al., *Liver and kidney metabolism during prolonged starvation.* The Journal of clinical investigation, 1969. **48**(3): p. 574-583.
51. Bobo, L., R.J. Womeodu, and A.L. Knox Jr, *Society of general internal medicine symposium principles of intercultural medicine in an internal medicine program.* The American journal of the medical sciences, 1991. **302**(4): p. 244-248.
52. Veech, R.L., *The therapeutic implications of ketone bodies: the effects of ketone bodies in pathological conditions: ketosis, ketogenic diet, redox states, insulin resistance, and*

mitochondrial metabolism. Prostaglandins, leukotrienes and essential fatty acids, 2004. **70**(3): p. 309-319.

53. Laffel, L., *Ketone bodies: a review of physiology, pathophysiology and application of monitoring to diabetes.* Diabetes/metabolism research and reviews, 1999. **15**(6): p. 412-426.
54. VanItallie, T.B. and T.H. Nufert, *Ketones: metabolism's ugly duckling.* Nutrition reviews, 2003. **61**(10): p. 327-341.
55. Krebs, H., *The regulation of the release of ketone bodies by the liver.* Advances in enzyme regulation, 1966. **4**: p. 339-353.
56. Robinson, A.M. and D.H. Williamson, *Physiological roles of ketone bodies as substrates and signals in mammalian tissues.* Physiological reviews, 1980. **60**(1): p. 143-187.
57. Bassenge, E., et al., *Effect of ketone bodies on cardiac metabolism.* American Journal of Physiology-Legacy Content, 1965. **208**(1): p. 162-168.
58. Fukao, T., et al., *Enzymes of ketone body utilization in human tissues: protein and messenger RNA levels of succinyl-coenzyme A (CoA): 3-ketoacid CoA transferase and mitochondrial and cytosolic acetoacetyl-CoA thiolases.* Pediatric research, 1997. **42**(4): p. 498-502.
59. Major, J.L., et al., *E2F6 impairs glycolysis and activates BDH1 expression prior to dilated cardiomyopathy.* PloS one, 2017. **12**(1): p. e0170066.
60. Sikder, K., et al., *High fat diet upregulates fatty acid oxidation and ketogenesis via intervention of PPAR-γ.* Cellular Physiology and Biochemistry, 2018. **48**(3): p. 1317-1331.
61. Wang, Y., et al., *The nitrated proteome in heart mitochondria of the db/db mouse model: characterization of nitrated tyrosine residues in SCOT.* Journal of proteome research, 2010. **9**(8): p. 4254-4263.
62. Taggart, A.K., et al., *(D)-β-hydroxybutyrate inhibits adipocyte lipolysis via the nicotinic acid receptor PUMA-G.* Journal of Biological Chemistry, 2005. **280**(29): p. 26649-26652.
63. Kimura, I., et al., *Short-chain fatty acids and ketones directly regulate sympathetic nervous system via G protein-coupled receptor 41 (GPR41).* Proceedings of the national academy of sciences, 2011. **108**(19): p. 8030-8035.

64. Xie, Z., et al., *Metabolic regulation of gene expression by histone lysine β-hydroxybutyrylation.* Molecular cell, 2016. **62**(2): p. 194-206.
65. Shimazu, T., et al., *Suppression of oxidative stress by β-hydroxybutyrate, an endogenous histone deacetylase inhibitor.* Science, 2013. **339**(6116): p. 211-214.
66. Newman, J.C. and E. Verdin, *Ketone bodies as signaling metabolites.* Trends in Endocrinology & Metabolism, 2014. **25**(1): p. 42-52.
67. Bae, H.R., et al., *β-Hydroxybutyrate suppresses inflammasome formation by ameliorating endoplasmic reticulum stress via AMPK activation.* Oncotarget, 2016. **7**(41): p. 66444.
68. Youm, Y.-H., et al., *The ketone metabolite β-hydroxybutyrate blocks NLRP3 inflammasome–mediated inflammatory disease.* Nature medicine, 2015. **21**(3): p. 263-269.
69. Taegtmeyer, H., *Genetics of energetics: transcriptional responses in cardiac metabolism.* Annals of biomedical engineering, 2000. **28**(8): p. 871-876.
70. Neubauer, S., et al., *Myocardial phosphocreatine-to-ATP ratio is a predictor of mortality in patients with dilated cardiomyopathy.* Circulation, 1997. **96**(7): p. 2190-2196.
71. Krahe, T., et al., *31P-cardio-MR-spectroscopy in myocardial insufficiency.* RoFo: Fortschritte auf dem Gebiete der Rontgenstrahlen und der Nuklearmedizin, 1993. **159**(1): p. 64-70.
72. Neubauer, S., *The failing heart—an engine out of fuel.* New England Journal of Medicine, 2007. **356**(11): p. 1140-1151.
73. Casademont, J. and Ò. Miró, *Electron transport chain defects in heart failure.* Heart failure reviews, 2002. **7**(2): p. 131-139.
74. Weiss, R.G., G. Gerstenblith, and P.A. Bottomley, *ATP flux through creatine kinase in the normal, stressed, and failing human heart.* Proceedings of the National Academy of Sciences, 2005. **102**(3): p. 808-813.
75. Fukushima, A., et al., *Myocardial energy substrate metabolism in heart failure: from pathways to therapeutic targets.* Current pharmaceutical design, 2015. **21**(25): p. 3654-3664.
76. Allard, M., et al., *Contribution of oxidative metabolism and glycolysis to ATP production in hypertrophied hearts.* American Journal of Physiology-Heart and Circulatory Physiology, 1994. **267**(2): p. H742-H750.

77. Zhang, L., et al., *Cardiac insulin-resistance and decreased mitochondrial energy production precede the development of systolic heart failure after pressure-overload hypertrophy.* Circulation: Heart Failure, 2013. **6**(5): p. 1039-1048.
78. HERRMANN, G. and G.M. DECHERD JR, *The chemical nature of heart failure.* Annals of Internal Medicine, 1939. **12**(8): p. 1233-1244.
79. OLSON, R.E. and W.B. SCHWARTZ, *Myocardial metabolism in congestive heart failure.* Medicine, 1951. **30**(1): p. 21-42.
80. Ho, K.L., et al., *Increased ketone body oxidation provides additional energy for the failing heart without improving cardiac efficiency.* Cardiovascular research, 2019. **115**(11): p. 1606-1616.
81. Masoud, W.G., A.S. Clanachan, and G.D. Lopaschuk, *The failing heart: is it an inefficient engine or an engine out of fuel?*, in *Cardiac Remodeling*. 2013, Springer. p. 65-84.
82. Jüllig, M., et al., *Is the failing heart out of fuel or a worn engine running rich? A study of mitochondria in old spontaneously hypertensive rats.* Proteomics, 2008. **8**(12): p. 2556-2572.
83. Simonsen, S. and J.K. Kjekshus, *The effect of free fatty acids on myocardial oxygen consumption during atrial pacing and catecholamine infusion in man.* Circulation, 1978. **58**(3): p. 484-491.
84. Mjøs, O.D., *Effect of free fatty acids on myocardial function and oxygen consumption in intact dogs.* The Journal of clinical investigation, 1971. **50**(7): p. 1386-1389.
85. Kintscher, U., et al., *The role of adipose triglyceride lipase and cytosolic lipolysis in cardiac function and heart failure.* Cell Reports Medicine, 2020. **1**(1): p. 100001.
86. Qi, D., et al., *Single-dose dexamethasone induces whole-body insulin resistance and alters both cardiac fatty acid and carbohydrate metabolism.* Diabetes, 2004. **53**(7): p. 1790-1797.
87. García-Rúa, V., et al., *Increased expression of fatty-acid and calcium metabolism genes in failing human heart.* PLoS One, 2012. **7**(6): p. e37505.
88. Coort, S.L., et al., *Enhanced sarcolemmal FAT/CD36 content and triacylglycerol storage in cardiac myocytes from obese zucker rats.* Diabetes, 2004. **53**(7): p. 1655-1663.

89. Paolisso, G., et al., *Total-body and myocardial substrate oxidation in congestive heart failure.* Metabolism, 1994. **43**(2): p. 174-179.
90. Taylor, M., et al., *An evaluation of myocardial fatty acid and glucose uptake using PET with [18F] fluoro-6-thia-heptadecanoic acid and [18F] FDG in patients with congestive heart failure.* Journal of Nuclear Medicine, 2001. **42**(1): p. 55-62.
91. Neglia, D., et al., *Impaired myocardial metabolic reserve and substrate selection flexibility during stress in patients with idiopathic dilated cardiomyopathy.* American Journal of Physiology-Heart and Circulatory Physiology, 2007. **293**(6): p. H3270-H3278.
92. Tuunanen, H., et al., *Response to Letters Regarding Article,"Free Fatty Acid Depletion Acutely Decreases Cardiac Work and Efficiency in Cardiomyopathic Heart Failure".* Circulation, 2007. **115**(21): p. e547-e547.
93. Dávila-Román, V.G., et al., *Altered myocardial fatty acid and glucose metabolism in idiopathic dilated cardiomyopathy.* Journal of the American College of Cardiology, 2002. **40**(2): p. 271-277.
94. Heather, L.C., et al., *Fatty acid transporter levels and palmitate oxidation rate correlate with ejection fraction in the infarcted rat heart.* Cardiovascular research, 2006. **72**(3): p. 430-437.
95. Grover-McKay, M., et al., *Regional myocardial blood flow and metabolism at rest in mildly symptomatic patients with hypertrophic cardiomyopathy.* Journal of the American College of Cardiology, 1989. **13**(2): p. 317-324.
96. Rosenblatt-Velin, N., et al., *Postinfarction heart failure in rats is associated with upregulation of GLUT-1 and downregulation of genes of fatty acid metabolism.* Cardiovascular research, 2001. **52**(3): p. 407-416.
97. Kato, T., et al., *Analysis of metabolic remodeling in compensated left ventricular hypertrophy and heart failure.* Circulation: Heart Failure, 2010. **3**(3): p. 420-430.
98. Jaswal, J.S., et al., *Targeting fatty acid and carbohydrate oxidation—a novel therapeutic intervention in the ischemic and failing heart.* Biochimica et Biophysica Acta (BBA)-Molecular Cell Research, 2011. **1813**(7): p. 1333-1350.
99. Mori, J., et al., *ANG II causes insulin resistance and induces cardiac metabolic switch and inefficiency: a critical role of PDK4.* American Journal of Physiology-Heart and Circulatory Physiology, 2013. **304**(8): p. H1103-H1113.

100. Zhabyeyev, P., et al., *Pressure-overload-induced heart failure induces a selective reduction in glucose oxidation at physiological afterload.* Cardiovascular research, 2013. **97**(4): p. 676-685.
101. Dutka, D.P., et al., *Myocardial glucose transport and utilization in patients with type 2 diabetes mellitus, left ventricular dysfunction, and coronary artery disease.* Journal of the American College of Cardiology, 2006. **48**(11): p. 2225-2231.
102. Nascimben, L., et al., *Mechanisms for increased glycolysis in the hypertrophied rat heart.* Hypertension, 2004. **44**(5): p. 662-667.
103. Dai, D.-F., et al., *Mitochondrial proteome remodelling in pressure overload-induced heart failure: the role of mitochondrial oxidative stress.* Cardiovascular research, 2012. **93**(1): p. 79-88.
104. Diakos, N.A., et al., *Evidence of glycolysis up-regulation and pyruvate mitochondrial oxidation mismatch during mechanical unloading of the failing human heart: implications for cardiac reloading and conditioning.* JACC: Basic to Translational Science, 2016. **1**(6): p. 432-444.
105. Bouillaud, F., M. Combes-George, and D. Ricquier, *Mitochondria of adult human brown adipose tissue contain a 32 000-M r uncoupling protein.* Bioscience Reports, 1983. **3**(8): p. 775-780.
106. Baartscheer, A., et al., *The driving force of the Na+/Ca2+-exchanger during metabolic inhibition.* Frontiers in physiology, 2011. **2**: p. 10.
107. McVeigh, J.J. and G.D. Lopaschuk, *Dichloroacetate stimulation of glucose oxidation improves recovery of ischemic rat hearts.* American Journal of Physiology-Heart and Circulatory Physiology, 1990. **259**(4): p. H1079-H1085.
108. Stanley, W.C., et al., *Pyruvate dehydrogenase activity and malonyl CoA levels in normal and ischemic swine myocardium: effects of dichloroacetate.* Journal of molecular and cellular cardiology, 1996. **28**(5): p. 905-914.
109. Jeffrey, F., et al., *Direct evidence that perhexiline modifies myocardial substrate utilization from fatty acids to lactate.* Journal of cardiovascular pharmacology, 1995. **25**(3): p. 469-472.

110. Kennedy, J.A., et al., *Effect of perhexiline and oxfenicine on myocardial function and metabolism during low-flow ischemia/reperfusion in the isolated rat heart.* Journal of cardiovascular pharmacology, 2000. **36**(6): p. 794-801.
111. Lopaschuk, G., et al., *Glucose and palmitate oxidation in isolated working rat hearts reperfused after a period of transient global ischemia.* Circulation research, 1990. **66**(2): p. 546-553.
112. Kantor, P.F., et al., *The antianginal drug trimetazidine shifts cardiac energy metabolism from fatty acid oxidation to glucose oxidation by inhibiting mitochondrial long-chain 3-ketoacyl coenzyme A thiolase.* Circulation research, 2000. **86**(5): p. 580-588.
113. Lopaschuk, G.D., et al., *Beneficial effects of trimetazidine in ex vivo working ischemic hearts are due to a stimulation of glucose oxidation secondary to inhibition of long-chain 3-ketoacyl coenzyme a thiolase.* Circulation research, 2003. **93**(3): p. e33-e37.
114. Dyck, J.R., et al., *Malonyl coenzyme a decarboxylase inhibition protects the ischemic heart by inhibiting fatty acid oxidation and stimulating glucose oxidation.* Circulation research, 2004. **94**(9): p. e78-e84.
115. Reszko, A.E., et al., *Regulation of malonyl-CoA concentration and turnover in the normal heart.* Journal of Biological Chemistry, 2004. **279**(33): p. 34298-34301.
116. Stanley, W.C., et al., *Malonyl-CoA decarboxylase inhibition suppresses fatty acid oxidation and reduces lactate production during demand-induced ischemia.* American Journal of Physiology-Heart and Circulatory Physiology, 2005. **289**(6): p. H2304-H2309.
117. Lommi, J., et al., *Blood ketone bodies in congestive heart failure.* Journal of the American College of Cardiology, 1996. **28**(3): p. 665-672.
118. Bedi Jr, K.C., et al., *Evidence for intramyocardial disruption of lipid metabolism and increased myocardial ketone utilization in advanced human heart failure.* Circulation, 2016. **133**(8): p. 706-716.
119. Voros, G., et al., *Increased cardiac uptake of ketone bodies and free fatty acids in human heart failure and hypertrophic left ventricular remodeling.* Circulation: Heart Failure, 2018. **11**(12): p. e004953.
120. Aubert, G., et al., *The failing heart relies on ketone bodies as a fuel.* Circulation, 2016. **133**(8): p. 698-705.

121. Schugar, R.C., et al., *Cardiomyocyte-specific deficiency of ketone body metabolism promotes accelerated pathological remodeling.* Molecular metabolism, 2014. **3**(7): p. 754-769.
122. Nielsen, R., et al., *Cardiovascular effects of treatment with the ketone body 3-hydroxybutyrate in chronic heart failure patients.* Circulation, 2019. **139**(18): p. 2129-2141.
123. Horton, J.L., et al., *The failing heart utilizes 3-hydroxybutyrate as a metabolic stress defense.* JCI insight, 2019. **4**(4).
124. Monzo, L., et al., *Myocardial ketone body utilization in patients with heart failure: The impact of oral ketone ester.* Metabolism, 2021. **115**: p. 154452.
125. Ferrannini, E., M. Mark, and E. Mayoux, *CV protection in the EMPA-REG OUTCOME trial: a "thrifty substrate" hypothesis.* Diabetes care, 2016. **39**(7): p. 1108-1114.
126. Mudaliar, S., S. Alloju, and R.R. Henry, *Can a shift in fuel energetics explain the beneficial cardiorenal outcomes in the EMPA-REG OUTCOME study? A unifying hypothesis.* Diabetes care, 2016. **39**(7): p. 1115-1122.
127. Verma, S., et al., *Empagliflozin increases cardiac energy production in diabetes: novel translational insights into the heart failure benefits of SGLT2 inhibitors.* JACC: Basic to Translational Science, 2018. **3**(5): p. 575-587.
128. Hattersley, A.T. and B. Thorens, *Type 2 diabetes, SGLT2 inhibitors, and glucose secretion.* New England Journal of Medicine, 2015. **373**(10): p. 974-976.
129. Gallo, L.A., E.M. Wright, and V. Vallon, *Probing SGLT2 as a therapeutic target for diabetes: basic physiology and consequences.* Diabetes and Vascular Disease Research, 2015. **12**(2): p. 78-89.
130. Nair, S. and J.P. Wilding, *Sodium glucose cotransporter 2 inhibitors as a new treatment for diabetes mellitus.* The Journal of Clinical Endocrinology & Metabolism, 2010. **95**(1): p. 34-42.
131. Levine, J.A., S.L. Karam, and G. Aleppo, *SGLT2-I in the hospital setting: diabetic ketoacidosis and other benefits and concerns.* Current diabetes reports, 2017. **17**(7): p. 1-8.
132. Bolinder, J., et al., *Effects of dapagliflozin on body weight, total fat mass, and regional adipose tissue distribution in patients with type 2 diabetes mellitus with inadequate*

glycemic control on metformin. The Journal of Clinical Endocrinology & Metabolism, 2012. **97**(3): p. 1020-1031.

133. Yokono, M., et al., *SGLT2 selective inhibitor ipragliflozin reduces body fat mass by increasing fatty acid oxidation in high-fat diet-induced obese rats.* European journal of pharmacology, 2014. **727**: p. 66-74.
134. Vallon, V. and S.C. Thomson, *Targeting renal glucose reabsorption to treat hyperglycaemia: the pleiotropic effects of SGLT2 inhibition.* Diabetologia, 2017. **60**(2): p. 215-225.
135. Zinman, B., et al., *Empagliflozin, cardiovascular outcomes, and mortality in type 2 diabetes.* New England Journal of Medicine, 2015. **373**(22): p. 2117-2128.
136. Neal, B., et al., *Canagliflozin and cardiovascular and renal events in type 2 diabetes.* New England Journal of Medicine, 2017. **377**(7): p. 644-657.
137. Wiviott, S.D., et al., *Dapagliflozin and cardiovascular outcomes in type 2 diabetes.* New England Journal of Medicine, 2019. **380**(4): p. 347-357.
138. McMurray, J.J., et al., *Dapagliflozin in patients with heart failure and reduced ejection fraction.* New England Journal of Medicine, 2019. **381**(21): p. 1995-2008.
139. Packer, M., et al., *Cardiovascular and renal outcomes with empagliflozin in heart failure.* New England Journal of Medicine, 2020. **383**(15): p. 1413-1424.
140. Shi, L., et al., *Dapagliflozin attenuates cardiac remodeling in mice model of cardiac pressure overload.* American journal of hypertension, 2019. **32**(5): p. 452-459.
141. Yurista, S.R., et al., *Sodium–glucose co-transporter 2 inhibition with empagliflozin improves cardiac function in non-diabetic rats with left ventricular dysfunction after myocardial infarction.* European journal of heart failure, 2019. **21**(7): p. 862-873.
142. Santos-Gallego, C.G., et al., *Empagliflozin ameliorates adverse left ventricular remodeling in nondiabetic heart failure by enhancing myocardial energetics.* Journal of the American College of Cardiology, 2019. **73**(15): p. 1931-1944.
143. Mazidi, M., et al., *Effect of sodium-glucose cotransport-2 inhibitors on blood pressure in people with type 2 diabetes mellitus: a systematic review and meta-analysis of 43 randomized control trials with 22 528 patients.* Journal of the American Heart Association, 2017. **6**(6): p. e004007.

144. Ferrannini, E., et al., *Renal handling of ketones in response to sodium–glucose cotransporter 2 inhibition in patients with type 2 diabetes.* Diabetes care, 2017. **40**(6): p. 771-776.
145. Prattichizzo, F., et al., *Increases in circulating levels of ketone bodies and cardiovascular protection with SGLT2 inhibitors: Is low-grade inflammation the neglected component?* Diabetes, Obesity and Metabolism, 2018. **20**(11): p. 2515-2522.
146. Lee, T.-M., N.-C. Chang, and S.-Z. Lin, *Dapagliflozin, a selective SGLT2 Inhibitor, attenuated cardiac fibrosis by regulating the macrophage polarization via STAT3 signaling in infarcted rat hearts.* Free Radical Biology and Medicine, 2017. **104**: p. 298-310.
147. Kang, S., et al., *Direct effects of empagliflozin on extracellular matrix remodelling in human cardiac myofibroblasts: novel translational clues to explain EMPA-REG OUTCOME results.* Canadian Journal of Cardiology, 2020. **36**(4): p. 543-553.
148. Byrne, N.J., et al., *Empagliflozin blunts worsening cardiac dysfunction associated with reduced NLRP3 (nucleotide-binding domain-like receptor protein 3) inflammasome activation in heart failure.* Circulation: Heart Failure, 2020. **13**(1): p. e006277.
149. Ferrannini, E., et al., *Shift to fatty substrate utilization in response to sodium–glucose cotransporter 2 inhibition in subjects without diabetes and patients with type 2 diabetes.* Diabetes, 2016. **65**(5): p. 1190-1195.
150. Ferrannini, E., et al., *Metabolic response to sodium-glucose cotransporter 2 inhibition in type 2 diabetic patients.* The Journal of clinical investigation, 2014. **124**(2): p. 499-508.
151. Al Jobori, H., et al., *Determinants of the increase in ketone concentration during SGLT2 inhibition in NGT, IFG and T2DM patients.* Diabetes, Obesity and Metabolism, 2017. **19**(6): p. 809-813.
152. Lambert, R., et al., *Intracellular Na+ concentration ([Na+] i) is elevated in diabetic hearts due to enhanced Na+–glucose cotransport.* Journal of the American Heart Association, 2015. **4**(9): p. e002183.
153. Ho, K.L., et al., *Ketones can become the major fuel source for the heart but do not increase cardiac efficiency.* Cardiovascular research, 2021. **117**(4): p. 1178-1187.
154. Mohammed, S.F., et al., *Variable phenotype in murine transverse aortic constriction.* Cardiovascular Pathology, 2012. **21**(3): p. 188-198.

155. Nakamura, A., et al., *LV systolic performance improves with development of hypertrophy after transverse aortic constriction in mice.* American Journal of Physiology-Heart and Circulatory Physiology, 2001. **281**(3): p. H1104-H1112.
156. Xia, Y., et al., *Characterization of the inflammatory and fibrotic response in a mouse model of cardiac pressure overload.* Histochemistry and cell biology, 2009. **131**(4): p. 471-481.
157. Uddin, G.M., et al., *Impaired branched chain amino acid oxidation contributes to cardiac insulin resistance in heart failure.* Cardiovascular diabetology, 2019. **18**(1): p. 1-12.
158. Chen, H., et al., *Dapagliflozin and ticagrelor have additive effects on the attenuation of the activation of the NLRP3 inflammasome and the progression of diabetic cardiomyopathy: an AMPK–mTOR interplay.* Cardiovascular drugs and therapy, 2020. **34**(4): p. 443-461.
159. Withaar, C., et al., *The effects of liraglutide and dapagliflozin on cardiac function and structure in a multi-hit mouse model of heart failure with preserved ejection fraction.* Cardiovascular Research, 2020.
160. Arow, M., et al., *Sodium–glucose cotransporter 2 inhibitor Dapagliflozin attenuates diabetic cardiomyopathy.* Cardiovascular diabetology, 2020. **19**(1): p. 1-12.
161. Li, C., et al., *SGLT2 inhibition with empagliflozin attenuates myocardial oxidative stress and fibrosis in diabetic mice heart.* Cardiovascular diabetology, 2019. **18**(1): p. 1-13.
162. Joubert, M., et al., *The sodium–glucose cotransporter 2 inhibitor dapagliflozin prevents cardiomyopathy in a diabetic lipodystrophic mouse model.* Diabetes, 2017. **66**(4): p. 1030-1040.
163. Mieczkowska, A., et al., *Dapagliflozin and Liraglutide therapies rapidly enhanced bone material properties and matrix biomechanics at bone formation site in a type 2 diabetic mouse model.* Calcified Tissue International, 2020. **107**(3): p. 281-293.
164. Tatarkiewicz, K., et al., *Combined antidiabetic benefits of exenatide and dapagliflozin in diabetic mice.* Diabetes, Obesity and Metabolism, 2014. **16**(4): p. 376-380.
165. Karwi, Q.G., et al., *Concurrent diabetes and heart failure: interplay and novel therapeutic approaches.* Cardiovascular Research, 2021.

166. Richards, D.A., et al., *Distinct phenotypes induced by three degrees of transverse aortic constriction in mice.* Scientific reports, 2019. **9**(1): p. 1-15.
167. Kemp, C.D. and J.V. Conte, *The pathophysiology of heart failure.* Cardiovascular Pathology, 2012. **21**(5): p. 365-371.
168. Crespo-Leiro, M.G., et al., *Advanced heart failure: a position statement of the Heart Failure Association of the European Society of Cardiology.* European journal of heart failure, 2018. **20**(11): p. 1505-1535.
169. Jackson, G., et al., *ABC of heart failure: Pathophysiology.* BMJ: British Medical Journal, 2000. **320**(7228): p. 167.
170. Walker, M.K., et al., *A less stressful alternative to oral gavage for pharmacological and toxicological studies in mice.* Toxicology and applied pharmacology, 2012. **260**(1): p. 65-69.